Kobe University Repository : Kernel

PDF issue: 2025-12-05

MpDWF5A-Encoded Sterol Δ7-Reductase Is Essential for the Normal Growth and Development of Marchantia polymorpha

Hatada, Miki
Akiyama, Ryouta
Yamagishi, Moeko
Ishizaki, Kimitsune
Mizutani, Masaharu

(Citation)
Plant and Cell Physiology,64(7):826-838

(Issue Date)
2023-05-11

(Resource Type)
journal article

(Version)
Accepted Manuscript

(Rights)
This is a pre-copyedited, author-produced version of an article accepted for publication in Plant and Cell Physiology following peer review. The version of record Miki Hatada, Ryota Akiyama, Moeko Yamagishi, Kimitsune Ishizaki, Masaharu Mizutani, MpDWF5A-Encoded Sterol Δ7-Reductase Is Essential for the Normal Growth and…

(URL)
https://hdl.handle.net/20.500.14094/0100489696

Mp*DWF5A*-encoded sterol Δ7-reductase is essential for the normal growth and development of *Marchantia polymorpha*

***Corresponding author:** Masaharu Mizutani

Graduate School of Agricultural Science, Kobe University

1-1 Rokkodai, Nada, Kobe 657-8501, Japan

Tel: 81-78-803-5885; Fax: 81-78-803-5884; E-mail: mizutani@gold.kobe-u.ac.jp

Subject Areas: proteins, enzymes and metabolism

The number of black and white figures: 4

The number of colored figures: 2

The number of tables: 1

The number of supplementary figures: 9

The number of supplementary tables: 5

The number of supplementary data sets: 0

Mp*DWF5A*-encoded sterol Δ7-reductase is essential for the normal growth and development of *Marchantia polymorpha*

Miki Hatada[1], Ryota Akiyama[1], Moeko Yamagishi[1], Kimitsune Ishizaki[2], Masaharu Mizutani[1]*

[1]Graduate School of Agricultural Science, Kobe University, 1-1 Rokkodai, Nada, Kobe, Hyogo 657-8501, Japan.

[2]Graduate School of Science, Kobe University, 1-1 Rokkodai, Nada, Kobe, Hyogo 657-8501, Japan.

*Corresponding author: Masaharu Mizutani

Graduate School of Agricultural Science, Kobe University

1-1 Rokkodai, Nada, Kobe 657-8501, Japan

Tel: 81-78-803-5885; Fax: 81-78-803-5884; E-mail: mizutani@gold.kobe-u.ac.jp

Running title:

Sterol Δ7-reductase in *Marchantia polymorpha*

Abstract

Sterols are the essential components of the eukaryotic cell membranes. However, studies on sterol biosynthesis in bryophytes are limited. This study analyzed the sterol profiles in the bryophyte model plant *Marchantia polymorpha* L. The thalli contained typical phytosterols such as campesterol, sitosterol, and stigmasterol. BLASTX analysis of the *M. polymorpha* genome against the *Arabidopsis thaliana* sterol biosynthetic genes confirmed the presence of all of the enzymes responsible for sterol biosynthesis in *M. polymorpha*. In this study, we focused on characterizing two genes, *MpDWF5A* and *MpDWF5B,* which showed high homology with *A. thaliana DWF5*, encoding Δ5,Δ7-sterol Δ7-reductase. Functional analysis using a yeast expression system revealed that MpDWF5A converted 7-dehydrocholesterol to cholesterol, indicating that MpDWF5A is a Δ5,Δ7-sterol Δ7-reductase. *Mpdwf5a*-knockout lines (*Mpdwf5a*-ko) were constructed using CRISPR/Cas9 mediated genome editing. GC-MS analysis of *Mpdwf5a*-ko revealed that phytosterols such as campesterol, sitosterol, and stigmasterol disappeared, and instead, the corresponding Δ7-type sterols accumulated. The thalli of *Mpdwf5a*-ko grew smaller than those of the wild type, and excessive formation of apical meristem in the thalli was observed. In addition, the gemma cups of the *Mpdwf5a*-ko were incomplete, and only a limited number of gemma formations were observed. Treatment with 1 μM of castesterone or 6-deoxocastasterone, a bioactive brassinosteroid, partly restored some of these abnormal phenotypes, but far from complete recovery. These results indicate that *MpDWF5A* is essential for the normal growth and development of *M. polymorpha* and suggest that the dwarfism caused by the *MpDWF5A* defect is due to the deficiency of typical phytosterols and, in part, a brassinosteroid-like compound derived from phytosterols.

Keywords:

Marchantia, sterol biosynthesis, sterol Δ7-reductase, brassinosteroid, DWF5

Introduction

Sterols are the essential components of the cell membranes for the survival of eukaryotes, and their composition varies among the taxonomic groups, with animals producing cholesterol and fungi producing ergosterol (Darnet *et al.* 2021). The main sterols produced by land plants include phytosterols such as campesterol, stigmasterol, and sitosterol, while algae produce a variety of sterols depending on the species (Dembitsky 1993; Girard *et al.* 2021; Voshall *et al.* 2021). The phytosterol biosynthetic capacity is essential for the terrestrialization strategy of plants. However, sterol biosynthesis in the early diverging lineages of land plants is largely unknown.

Phytosterols are present in free or conjugated forms, such as sterol esters and sterol glycosides. Free sterols are the most abundant form of phytosterols. They are integral components of the membrane lipid bilayer, where they interact with other membrane components and play a functional role in regulating membrane fluidity and permeability (Demel and De Kruyff, 1976; Roche *et al.*, 2008). Modification of the plant sterol content in the plasma membrane affects on the function of membrane-bound proteins' function, including the enzymes, channels, and receptors or other components of the signal transduction pathways (Grandmougin-Ferjani *et al.*, 1997; Carland *et al*., 2010). Maintenance of the amount and the composition ratio of free sterols is essential for developing plants. Sterol esters, which are esterified at the C3-hydroxy group, play a central role in the membrane sterol homeostasis and represent a storage pool of sterols in particular plant tissues (Shimada *et al.*, 2019). Sterol glycosides, which are glycosylated at the C3-hydroxy group, are one of the significant components of the plasma membrane and accumulate specifically in the lipid rafts, which are known to mediate many cellular processes (Ferrer *et al.*, 2017). Biosynthesis of sterols begins from the squalene biosynthesis via the mevalonate pathway (Figure 1). The committed precursor for the phytosterols (C-24 alkyl phytosterols) is cycloartenol, which is generated by cycloartenol synthase. Unlike plants, animals and fungi use lanosterol, generated by lanosterol synthase, as a committed precursor to generate cholesterol and ergosterol, respectively. The functions of enzymes involved in sterol biosynthesis are conserved in the eukaryotes (Supplementary Table S1). The difference in the end-products between plants and yeasts is due to the presence of three enzymes, cyclopropylsterol isomerase, sterol C28-methyltransferase, and Δ5,Δ7-sterol Δ7-reductase (hereafter abbreviated as C7R), which are present only in plants and result in the accumulation of the significant phytosterols such as C28-methysterol campesterol, C29-

ethylsterols, stigmasterol, and sitosterol. Moreover, campesterol is the precursor of the plant growth hormone brassinosteroid (BR).

Arabidopsis thaliana sterol-deficient mutants, such as *smt1/cph/orc* (Diener *et al*., 2000; Willemsen *et al*., 2003), *cpi1-1* (Men *et al*., 2008), *fackel/hydra2* (Jang *et al.*, 2000; Schrick *et al.*, 2000), and *hydra1* (Souter *et al*., 2002), which are defective in the genes involved in sterol biosynthesis upstream of 24-methylenelophenol (Figure 1 and Supplementary Table S1), exhibit severe dwarfism and abnormal development. These phenotypes are due to the impaired cell division and auxin transport, and, however, are distinct from the BR deficiency, as the exogenous application of BRs cannot rescue them. In contrast, *A. thaliana* mutants with the defects in the later steps of sterol biosynthetic genes that act downstream of avenasterol and episterol exhibit a typical BR deficient phenotype. *A. thaliana dwarf7* (*dwf7*) (Choe *et al*., 1999a) and *dwarf1/diminuto* (*dwf1/dim*) (Choe *et al.* 1999b; Klahre *et al*. 1998) are defective in the genes encoding Δ7-sterol C5-desaturase and Δ5-sterol Δ24-reductase, respectively, and these enzymes are involved in the biosynthesis of campesterol, the precursor of BR. These mutants exhibit dwarfism, and the exogenous BR can rescue such dwarf phenotypes. The *A. thaliana dwarf5* (*dwf5*) mutant also shows a small dark-green dwarf phenotype as a consequence of the BR deficiency, and *DWF5* has been identified to encode C7R, which is located between DWF7 and DWF1 in the biosynthesis of phytosterols and BR (Choe *et al*., 2000). In addition, *A. thaliana dwf5* accumulates the Δ7-sterols, particularly Δ7-sitosterol, and the irradiation by UV-B light causes the conversion of Δ7-sitosterol to accumulate vitamin D_5 in *A. thaliana* (Silvestro *et al*., 2018).

In the present study, we analyzed the sterol profiles in a bryophyte model plant *Marchantia polymorpha* L. and confirmed the presence of all enzymes responsible for sterol biosynthesis in the *M. polymorpha* genome. Among the sterol biosynthetic genes, we characterized *MpDWF5A*, encoding C7R. The *Mpdwf5a* mutant generated by CRISPR-Cas9-mediated genome editing exhibited loss of the typical phytosterols and accumulation of the corresponding Δ7-sterols and also showed dwarfism, which exogenous feeding of castasterone or 6-deoxocastasterone could partly rescue. According to these results, we discussed the essential function of *MpDWF5A* in the normal development of *M. polymorpha.*

Results

Sterol profile in *M. polymorpha*

To characterize sterol biosynthesis in *M. polymorpha*, the profile of sterol composition of the thallus of *M. polymorpha* was analyzed by GC-MS. The thalli comprised typical C_{28}-phytosterol, campesterol, C_{29}-phytosterols, sitosterol and stigmasterol, and only a trace amount of C_{27}-phytosterol cholesterol as free forms (Figure 2 and Table 1). The contents of esterified sterols were estimated after hydrolysis by saponification, and their contents were not significantly different from those before saponification (Table 1), suggesting that very few esterified sterols are present in *M. polymorpha*. To search for the genes involved in sterol biosynthesis in *M. polymorpha*, BLASTX analysis against the *M. polymorpha* protein database (https://marchantia.info) was performed using the ORF sequences encoded by the sterol biosynthetic genes in *A. thaliana* as queries. Supplementary Table S1 summarizes the results of the sterol biosynthetic enzymes in *M. polymorpha*. The *M. polymorpha* genome contains all of the enzymes responsible for sterol biosynthesis, showing 50%-70% amino acid sequence identity to the corresponding *A. thaliana* enzymes. *A. thaliana* has lanosterol synthase and cycloartenol synthase, whereas *M. polymorpha* has only cycloartenol synthase. More notably, the two reductases, C7R and Δ5-sterol 24-reductase, which are involved in the final steps of sterol biosynthesis, were present in two genes in *M. polymorpha*, compared to one gene in *A. thaliana*. In this study, we focused on characterizing two putative *C7R* genes in *M. polymorpha*.

Characterization of C7R in *M. polymorpha*

Two C7R candidates in *M. polymorpha* were identified as Mp2g07930 and Mp4g18020, which showed 69% and 50% amino acid sequence identity with *A. thaliana* DWF5 and were designated as MpDWF5A and MpDWF5B, respectively. The expression levels of the two candidate genes in the various tissues of *M. polymorpha* in the transcriptome data reported by Bowman *et al*. (2017) revealed that *MpDWF5A* was expressed throughout the body, whereas *MpDWF5B* was barely expressed except in the male organs and sporangia (Supplementary Table S2). A phylogenetic analysis was performed using the amino acid sequences of C7Rs from human, algae, and land plants (Figure 3). There are two or more *C7R* homologous genes in bryophytes. However, only one gene is present in the

model lycophyte *Selaginella moellendorffii* and one or no gene is present in green alga. C7R homologs from the bryophytes are divided into two clades: one contains C7Rs from seed plants and putative C7Rs from the ferns and the bryophytes including MpDWF5A, and the other consists of C7R homologs only from the bryophytes, including MpDWF5B. To analyze the enzymatic functions of MpDWF5A and MpDWF5B, each recombinant enzyme was expressed in yeast (GIL77). The crude enzymes prepared from the yeast cells expressing MpDWF5A converted 7-dehydrocholesterol to cholesterol, while the MpDWF5B crude enzymes did not. These results confirmed that MpDWF5A exhibited the sterol Δ7-reduction activity (Supplementary Figure S1).

Sterol profile in *Mpdwaf5a-ko*

To elucidate the *in vivo* function of *MpDWF5A* in *M. polymorpha*, *MpDWF5A* was disrupted using CRISPR/Cas9-mediated genome editing. By using the MpGE010 vector containing three gRNAs designed in the third exon of *MpDWF5A*, several lines of transgenic *M. polymorpha* were obtained and the analysis of the mutations in the region surrounding the gRNA target sites revealed a 34–43 base deletion in the third exon (Supplementary Figure S2A). The *Mpdwf5a* knockout lines (hereafter abbreviated as *Mpdwaf5a-ko* lines: #5-13, #32-15, and #47-2) showed a dwarf phenotype with a disorganized branching of the thalli (Supplementary Figure S2B). The thalli from the vector control strain and the *Mpdwaf5a-ko* lines grown for five weeks were extracted with 0.4 mL of $CHCl_3$:methanol (1:1), and GC-MS was used to analyze the resultant extracts to determine their sterol profiles. In the control strain, typical phytosterols such as campesterol, stigmasterol, and sitosterol were detected (peaks 1, 2, and 3 in Figure 4A, respectively), whereas the peaks corresponding to these phytosterols disappeared in the *Mpdwaf5a-ko* lines (Figure 4). Instead, three new peaks (peaks 4, 5, and 6 in Figure 4A) were detected 0.4–0.5 min in succession, corresponding to the three phytosterols. Since the difference in the retention time between cholesterol and 7-dehydrocholesterol is approximately 0.4 min, these new peaks were assumed to be the Δ7- forms of the corresponding phytosterols. To confirm, the mass spectra of the new peaks detected in the *Mpdwaf5a-ko* #47-2 line were compared with those of the peaks obtained from the standard phytosterols (Supplementary Figure S3). The parent molecular masses of the new peaks (peak 4, 470; peak 5, 482; and peak 6, 484) were two mass smaller than those of the standards (campesterol, 472; stigmasterol, 484; and sitosterol, 486), respectively,

indicating that the *Mpdwaf5a-ko* line accumulates the Δ7-type sterols. In addition, the fragmentation patterns of the new peaks were similar to that of 7-dehydrocholesterol, and the masses of their fragments were larger by the difference in the masses of the sterol side chains between 7-dehydrocholesterol and the phytosterols (campesterol, 14; stigmasterol, 26; sitosterol, 28). These results indicated that the new peaks 4, 5, and 6 are those of Δ7-campesterol, Δ7-stigmasterol, and Δ7-sitosterol, respectively. Thus, the mutation of *MpDWF5A* resulted in the accumulation of Δ7-sterols, indicating that *MpDWF5A* is involved in the Δ7 reduction of Δ5,Δ7-sterols in sterol biosynthesis in *M. polymorpha*. Next, quantitative analysis of the 7-dehydrosterols accumulated in the *Mpdwaf5a-ko* lines was performed (Figure 4B). The content of Δ7-campesterol in the *Mpdwaf5a-ko* lines was not significantly different from that of campesterol in the control. In contrast, the *Mpdwaf5a-ko* lines showed decreased Δ7-stigmasterol and increased Δ7-sitosterol contents compared to the stigmasterol and sitosterol contents in the vector control, suggesting that the low activity of MpCYP722 catalyzing a sterol 22-desaturase for Δ7-sitosterol may result in less efficient 22-desaturation of Δ7-sitosterol to Δ7-stigmasterol in the *Mpdwaf5a-ko* lines.

Phenotype of *Mpdwaf5a-ko*

Mpdwaf5a-ko (#5-13, #32-5, and #47-2) exhibited a dwarf phenotype in comparison to the control (Figure 5). The whole body of 28-day-old *Mpdwaf5a-ko* #47-2 was notably smaller than the control (Figures 5A and 5B), and the dwarf phenotype of *Mpdwaf5a-ko* was the result of a significantly reduced growth rate in comparison to the control (Supplementary Figure S4). The control exhibited growth with two branches originated from the apical meristem situated at the tip of the thalli, whereas *Mpdwaf5a-ko* exhibited three or more branches at the tip (Figures 5A and 5B). The abnormal dwarf phenotype of 72-day-old *Mpdwaf5a-ko* #47-2 was even more pronounced in comparison to the 56-day-old control (Figures 5C and 5D). At 28 days of age, *Mpdwaf5a-ko* lines (#5-13, #32-5, and #47-2) had significantly lower weight and leaf area than the control (Figures 5E and 5F), and furthermore, the number of gemma cups formed in the control was 38.1 ± 3.51 per individual, whereas the number of gemma cups formed in *Mpdwaf5a-ko* ranged from 0 to 3 per individual (Figure 5G).

Next, we examined the detailed phenotypes of the 28-day-old thalli of *Mpdwaf5a-ko* #47-2. The abnormal meristems of *Mpdwaf5a-ko* #47-2 formed from the outside of the tip (indicated by red triangles in Figure

6D), but not seen in the control (Figure 6A). Analysis of the section of the apical meristem sliced along the midrib revealed that *Mpdwaf5a-ko* had an enlarged apical tip, multiple meristem formation at the ventral, and inhibition of the ventral scale formation (Figure 6E) in comparison to the control (Figure 6B). The gemma cups of *Mpdwaf5a-ko* exhibited morphological abnormalities with a shorter rim and narrower gemma cup floor (Figure 6F) compared to the control (Figure 6C).

Subsequently, staining the tips of thallus with toluidine blue, which stains the ventral scale and rhizoids, was performed (Figure 6G and 6I). In the control, the ventral scales were arranged in rows along the costa, and rhizoids were formed in bundles from the ventral scale of the row nearest to the costa (Figure 6G and 6H). On the other hand, *Mdwarf5-ko* exhibited no row formation of the ventral scales and had only a few rhizoids (Figure 6I and 6J). Moreover, an anomalous tissue, not seen in the control, was found on the ventral side of *Mdwarf5-ko* (indicated by red lines in Figure 6J), and renaissance staining revealed that this tissue was an abnormal meristem (Figure 6K).

When the *Mpdwf5a-ko* mutant was complemented by constitutively expressing *MpDWF5A*, its abnormal phenotypes were restored to a level similar to that of the wild-type plant (Supplementary Figure S5A). The complemented lines (*Mpdwf5a-ko* #47/*MpDWF5A-ox* #1 and #3) recovered to the same level as the control in terms of leaf area and the number of gemma cup (Supplementary Figure S5C). GC-MS analysis also confirmed the presence of typical phytosterols and absence of Δ7-type sterols in the complemented plants (Supplementary Figure S6). These findings indicate that *MpDWF5A* is responsible for the reduction reaction at the 7-position of sterols, which is indispensable for the normal growth and development of *M. polymorpha*.

Effect of exogenous application of sterols and BRs on the *Mpdwaf5a-ko* phenotype

In angiosperms, a dwarf phenotype caused by BR deficiency can be rescued by applying bioactive BRs. Feeding experiments were performed on *Mpdwaf5a-ko* by growing them on agar medium containing castasterone (0.1-1 μM) for 14 days. The treatment of *Mpdwaf5a-ko* with 0.1–1 μM castasterone partially suppressed the excessive branching of the thalli and the dwarfism (Supplementary Figure S7A–D), and the treatment with 1 μM castasterone partially restored the ventral scale formation (Supplementary Figure S7I–J). However, the recovery observed in

Mpdwaf5a-ko with the castasterone treatment was far from complete in terms of the dwarfism, morphological abnormalities, and reduced number of gemma cups (Supplementary Figure S7A–D).

Next, feeding experiments with campesterol, stigmasterol, and 6-deoxocastasterone (1 μM each) were conducted to characterize the effects of their exogenous application on the *Mpdwaf5a-ko* phenotypes. Due to the low solubility of sterols and their poor uptake by the plants, the compounds were dissolved in 0.09% (w/v) 2-hydroxypropyl-β-cyclodextrin. In the feeding experiments, the solution (1 μM each) was layered over the entire thalli and removed after 5 min. This treatment was conducted every 4 days, and the phenotypes (thalli area, weight, and the number of cup) were observed after 18 days (Supplementary Figure S8). The *Mpdwf5a-ko* lines treated with 6-deoxocastasterone showed an increase in thalli area, weight, and the number of cups compared to the mock-treated lines but were far from complete recovery (Supplementary Figure S9C). The treatment of campesterol or stigmasterol to the *Mpdwf5a-ko* lines also resulted in slight increases in weight or thalli area, respectively (Supplementary Figure S9C). Thus, the exogenous application of phytosterols or BRs only partially but not completely restored some of the abnormal phenotypes of the *Mpdwf5a-ko* lines, and the phenotypes that were restored differed from compound to compound.

Discussion

M. polymorpha contains campesterol, sitosterol, and stigmasterol in their free forms, and the results are consistent to the previous report for the identification of typical phytosterols in the cultured cells of *M. polymorpha* (Park et al., 1999). All the enzymes involved in their biosynthesis are present in the *M. polymorpha* genome, and notably, we found two genes (*MpDWF5A* and *MpDWF5B*) presumably encoding C7R in *M. polymorpha*, whereas most of the seed plants, including *A. thaliana*, have one *C7R* gene. Solanaceae produces cholesterol-derived steroidal glycoalkaloids and possesses duplicated sterol biosynthesis genes, including the two *C7R* genes, and such duplicated genes are involved predominantly in cholesterol metabolism (Sonawane *et al.*, 2016). In contrast, we found that *M. polymorpha* contains a small amount of cholesterol and that MpDWF5B does not possess the C7R activity, suggesting that MpDWF5B is not involved in sterol biosynthesis. In bryophytes, two or more *C7R* homologous genes are present in the two phylogenetic clades, and MpDWF5B is included in the clade consisting

only of bryophyte C7Rs (Figure 3). These results suggest that diversification of *C7R*s occurred specifically in the bryophyte lineage, and the C7R homologs in the bryophyte-specific clade including MpDWF5B might be involved in a reduction reaction of an unknown metabolic pathway specific to the bryophyte lineage. The disruption of the *MpDWF5B* gene and characterization of the phenotype may help us to understand its function in *M. polymorpha*.

The sterol composition of the *Mpdwf5a-ko* mutant analyzed by GC-MS revealed the absence of the typical phytosterols campesterol, stigmasterol, and sitosterol observed in the vector control strain; instead, their corresponding Δ7-type sterols were detected (Figure 4). This proves that MpDWF5A catalyzing the 7-position reduction reaction is actually essential for sterol biosynthesis in *M. polymorpha*. *Mpdwf5a-ko* showed several abnormal morphological phenotypes, including dwarfism, excessive apical meristem formation, reduced gemma cups, dwarfing of the gemma cup rims, and inhibition of ventral scale formation (Figures 5 and 6). The abnormal phenotypes of *Mpdwf5a-ko* are similar to those observed in the *Mpbes1* knockout mutant (Mecchia *et al.*, 2021). *A. thaliana* BRI1-EMSSUPRESSOR1 (AtBES1)/*A. thaliana* BRASSINAZOLE RESISTANT1 (AtBZR1) is a transcription factor that plays a significant role in the BR signal transduction pathway (Wang *et al.*, 2002; Yin *et al*., 2002; He *et al.*, 2005), and MpBES1 in *M. polymorpha* is the closest homolog to AtBES1/AtBZR1. Mecchia *et al.* (2021) reported that impaired MpBES1 function disrupts cell proliferation and differentiation; the *Mpbes1* mutant showed dwarfism, no differentiation of the gemma cup and gemma, and inhibition of the ventral scale formation. The similarity between the *Mpbes1* mutant and *Mpdwf5a-ko* suggested that the *Mpdwf5a-ko* phenotype is partly due to a deficiency of a BR-like steroidal compound, which may be involved in MpBES1-dependent signal transduction pathway. Indeed, the exogenous application of 0.1–1 μM castasterone or 1 μM 6-deoxocastasterone to *Mpdwf5a-ko* partially restored its abnormal morphology (Supplementary Figures S7, S8, S9). Because the administration of phytosterols also restored dwarfism to some extent (Supplementary Figure S9), the abnormal phenotype of *Mpdwf5a-ko* may result from a deficiency of both phytosterols and a BR-like compound. However, the degree of recovery by these feeding experiments is far from complete. It is very challenging to restore the phenotype by feeding experiments because these compounds are highly hydrophobic and therefore are not fully absorbed by the plant or translocated in the tissues where the compounds are needed.

In bryophytes, including *M. polymorpha*, the presence of BRs is reported although their concentration

is lower than those in angiosperms, and most BR intermediates found in angiosperms were not detectable or only present at very low levels (Yokota *et al*., 2017). With respect to BR biosynthetic enzymes, *M. polymorpha* lacks cytochrome P450 monooxygenases (CYPs) in the family of CYP85 and CYP90 (Supplementary Table S3) (Yokota *et al.* 2017; Cannell *et al.* 2020), and the phenotype of the wild type is not affected by the treatment of brassinazole, an inhibitor of CYP90B (Mecchia *et al.* 2021). These results recall the possibility that an unknown steroidal compound, other than typical BRs, is present in *M. polymorpha*, which may function as a growth regulator. Recently, similar examples have been reported for a gibberellin-like compound (*ent*-3β-hydroxy-kaurenoid acid) in the moss *Physcomitrium patens* (Nakajima et al., 2020) as well as a strigolactone-like compound (bryosymbiol) in the bryophyte *Marchantia paleacea* (Kodama et al., 2022). As for the genes involved in the BR signal transduction, a sequence homologous to the *A. thaliana* BR receptor BRI1 is absent in *M. polymorpha*, but several genes of the downstream components, including *BES1*, *BSK*, and *BIN2*, are present (Supplementary Table S4) (Ferreira-Guerra et al. 2020; Furumizu and Sawa 2021). Therefore, it is most likely that *M. polymorpha* requires a BR-like bioactive compound derived from the *MpDWF5A*-dependent sterol pathway for the normal growth and development via a signal transduction pathway similar to that conserved in angiosperms. However, the mechanism of its biosynthesis and reception in *M. polymorpha* is unknown.

In summary, *MpDWF5A,* responsible for the sterol 7-position reduction reaction, is essential for sterol biosynthesis and the normal growth of *M. polymorpha*. This study is the first report to reveal that the *MpDWF5A* defect causes dwarfism due to the deficiency of phytosterols and, in part, a BR-like steroidal compound in bryophytes. Therefore, it will be essential to search for a bioactive steroidal compound in *M. polymorpha* by a bioassay-based purification in order to elucidate its biosynthesis and the signaling pathway in nonvascular plants.

Materials and methods

Plant materials

Marchantia polymorpha L. subsp. *ruderalis* accession Takaragaike-1 (Tak-1) was used (Ishizaki et al., 2008). The gemmae were grown on half-strength Gamborg-B5 in solidified with 1% agar at 22 °C under continuous white LED light (34–58 μmol/m^2 s) in plant thermostatic chambers.

Chemicals

Campesterol, stigmasterol, and β-sitosterol were purchased from Tama Biochemical Co., Ltd. (Tokyo, Japan). Cholesterol and 7-dehydrocholesterol were procured from Sigma-Aldrich (St. Louis, MO, USA). Castasterone was kindly provided by Brassino Co., Ltd. (Toyama, Japan). 6-deoxocastasterone was obtained as described previously (Ohnishi *et al.*,2006).

Exploration of sterol biosynthesis genes in M. polymorpha

For investigating the candidate sterol biosynthesis genes in *M. polymorpha*, BLASTX analysis was performed against the transcript database from MarpolBase (https://marchantia.info/). The analysis was performed using the ORF sequences of the sterol biosynthesis genes in *Arabidopsis* listed in Table 1. The ORF sequences of *Arabidopsis* sterol biosynthesis genes were acquired from the genomic database of TAIR (https://www.arabidopsis.org/index.jsp). The values of Fragments Per Kilobase of exon per Million mapped reads (FPKM) (Supplementary Table S2) were calculated as previously described (Bowman *et al*., 2017).

Phylogenetic analysis

For phylogenetic analysis of C7Rs, amino acid sequences were collected from the following databases: *M. polymorpha* from MarpolBase (http://marchantia.info/); *H.sapience* from the National Center for Biotechnology Information's reference sequence database (https://www.ncbi.nlm.nih.gov/refseq/); and *Porphyra umbilicalis*, *Coccomyxa subellipsoidea* C-169, *Botryococcus brauni*, *Micromonas pusilla* CCMP1545, *Ceratodon purpureus GG1*, *Physcomitrella patens*, *Sphagnum fallax*, *Sphagnum magellanicum*, *Selaginella moellendorffi*i, *Ceratopteris richardii*, *Thuja plicata*, *Amborella trichopoda*, *Cinnamomum kanehirae*, *Nymphaea colorata*, *Solanum lycopersicum*, *Solanum tuberosum*, *Oryza sativa* and *Arabidopsis thaliana* from the Phytozome (https://phytozome.jgi.doe.gov/pz/portal.html). Sequence alignments were performed using the MUSCLE program (Edgar, 2004), and the neighbor-joining tree was inferred in the MEGA10 (Kumar *et al*., 2018). Bootstrap analyses were performed by resampling one thousand sets.

Expression of the recombinant MpDWF5A and MpDWF5B in yeast

The DNA fragments containing the ORF sequences of the *MpDWF5A* and *MpDWF5B* genes were synthesized by adding the BamHI site at the 5'-end and the XhoI site at the 3'-end (Eurofins Genomics, Tokyo, Japan). The *MpDWF5A* and *MpDWF5B* ORFs were cloned into the pYES2 vector (Invitrogen, MA, USA) between the BamHI and XhoI sites. The yeast strain GIL77 was transformed with each of the constructed pYES2 vectors. According to the manufacturers' protocols, yeast transformation was performed using a Frozen-EZ Yeast Transformation II Kit (Zymo Research, CA, USA). The intact pYES2 vector was transformed into GIL77 as the empty vector control. The transformants were cultured in the yeast synthetic complete medium containing 2% (w/v) glucose, 10 μg/mL campesterol, 13μg/mL hemin (Tokyo Chemical Industry Co., Ltd. Tokyo, Japan), 1.2% (v/v) ethanol, and 0.3% (v/v) Tween-80, supplemented with -Ura DO supplement (Takara Bio Inc., Shiga, Japan) for one day at 30°C. The cells were transferred to a new medium of the same composition with 2% (w/v) galactose instead of glucose to induce the recombinant MpDWF5A and MpDWF5B and cultured for two days.

In vitro assay

The cultured yeast cells were collected and washed three times with the wash buffer (20 mM Tris-HCl (pH 7.5) and 50 mM NaCl) and suspended in buffer A (20 mM Tris-HCl (pH 7.5) 5% (v/v) glycerol, 1 mM ethylenediaminetetraacetic acid (EDTA), and 0.1 mM dithiothreitol). The cells were lysed using acid-washed glass beads (Sigma-Aldrich) at 4 °C, and cell debris was removed by centrifugation at 3,000 rpm for 15 min at 4 °C. The supernatant was used for further *in vitro* assays. The MpDWF5A and MpDWF5B assays were performed using a 400 μL reaction mixture comsisting of 100 mM Tris-HCl (pH 7.5), 20.5 mM EDTA, 1 mM NADPH as a coenzyme, 12.5 μM 7-dehydrocholesterol as a substrate, and the supernatant containing MpDWF5A or MpDWF5B. All the reactions were performed at 30 °C for 20 h and were terminated by adding 300 μL of hexane:ethyl acetate (4:1). The reaction products were extracted three times with an equal volume of hexane:ethyl acetate (4:1), and the organic phase was collected and dried under a flow of nitrogen gas. The residues were analyzed by gas chromatography–mass spectroscopy (GC-MS). The GC-MS conditions were set as shown in the

GC-MS section. Total ion chromatogram of MS scan mode (*m/z* 50-700) and selected ion monitoring (SIM) of m/z 129 were recorded. Cholesterol was monitored in the SIM mode chromatogram at *m/z* 129, respectively.

Sterol extraction from M. polymorpha

Eighteen-day-old Tak-1 thalli were used to determine the sterol profile in *M. polymorpha*, 35-day-old *Mpdwf5-ko* thalli and vector control thalli, and 28-day-old *MpDWF5A*-ox/ *Mpdwf5-ko* thalli and vector control thalli were used for comparing the sterol composition and amount in each strain. The thalli (ca. 100 mg fresh weight) were collected into a snap-cap tube (2 mL) and snap-frozen with liquid nitrogen with a zirconia bead (5 mm i.d.). After powdering with a beads cell-disrupter (at 1,800 rpm for 4 min, Mixer Mill MM 400, Verder Scientific Co., Ltd.), the thalli were extracted three times with 0.4 mL of $CHCl_3$:methanol (1:1). At the time of initial extraction, 25-hydroxycholesterol (Sigma-Aldrich) (1 μg) was added as the internal standard. The crude extractions were dried using a centrifugal evaporator and redissolved in 33.3% (v/v) ethanol. To hydrolyze esterified sterols in Tak-1, dried crude extractions were saponified with 0.4 mL of 20% (w/v) KOH in 33.3% (v/v) ethanol for one day at room temperature. The redissolved crude mixture and saponified mixture were extracted three times with 0.4 mL of hexane:ethyl acetate (4:1), and each organic solvent layer was evaporated to dryness. The samples were analyzed using GC-MS method.

GC-MS analysis

The sterol samples were trimethylsilylated by MSTFA (Thermo Scientific™, MA, USA) and subjected to GC-MS analysis. The GC-MS analyses were performed under the following conditions: GC-MS-QP2010 Ultra (Shimadzu, Kyoto, Japan) equipped with a DB-1MS (30 m × 0.25 mm, 0.25 μm film thickness; J&W Scientific, CA, USA) capillary column. The column temperature was set as follows: 80 °C for 1 min, raised to 300 °C at a rate of 20 °C/min, and held at 300 °C for 20 min. The interface temperature was 300 °C, and both the injector and ion source temperatures were 250 °C. The carrier gas (He) was delivered at a pressure of 103.8 kPa. A splitless injection was used with a 1 min sampling time. The mass spectrometer was operated in the electron impact mode with an ionization energy of 70 eV. To explore the sterol profile in *M. polymorpha*, both MS scan mode (*m/z* 50-

700) and SIM were used. A mass range of SIM was selected from qualifier ions of cholesterol (*m/z* 129 and 329), campesterol (*m/z* 73, 129 and 343), stigmasterol (*m/z* 83 and 129), β-sitosterol (*m/z* 73 and 129), and 25-hydroxycholesterol (*m/z* 131). The amounts of each sterol were determined using the relative area ratio of each sterol peak area against the 25-hydroxycholesterol (internal standard) peak area in the SIM chromatogram.

For the determination of the sterol profile in *Mpdwf5-ko*, an MS scan mode (*m/z* 50-700) was used. For the quantification of Δ^7-phytosterols in *Mpdwf5a-ko*, a mass range of SIM was selected from the qualifier ions of typical sterols (*m/z* 129), 7-dehydrocholesterol (*m/z* 325 and 351), Δ^7-campesterol (*m/z* 339 and 365), Δ^7-stigmasterol (*m/z* 351 and 377), Δ^7-β-sitosterol (*m/z* 353 and 379), and 25-hydroxycholesterol (*m/z* 131). The SIM chromatogram constructed a calibration curve of 7-dehydrocholesterol with 25-hydroxycholesterol as the internal standard. The amount of each Δ^7-phytosterol was assigned as 7-dehydrocholesterol equivalent. To explore the sterol profile in *MpDWF5A*-ox/ *Mpdwf5-ko*, both MS scan mode (*m/z* 50-700) and SIM were used. A mass range of SIM was selected the same range used for quantification of Δ^7-phytosterols in *Mpdwf5a-ko*.

Knockout of MpDWF5A

The knockout plants for *MpDWF5A* were generated by targeted genome editing using the CRISPR/Cas9 system. To design a gRNA target with a low off-target effect in *MpDWF5A*, we conducted *in silico* analyses using the Web tool Design sgRNAs for CRISPick (https://portals.broadinstitute.org/gppx/crispick/public) and Cas-OT software (Xiao *et al.*, 2014). We selected the target sequences named MpDWF5Ako_1824-1843, MpDWF5Ako_1830-1850, and MpDWF5Ako_1878-1897 in the genome sequence of *MpDWF5A*, respectively. To enhance the efficiency of gRNA transcription from the U6 promoter, one G was added to the 5'-end of MpDWF5Ako_1824-1843, MpDWF5Ako_1830-1850, and MpDWF5Ako_1878-1897. Two DNA fragments composed of the gRNA scaffold and the tRNA scaffold between two target sequences, MpDWF5Ako_1830-1850/half of the 5'-end of MpDWF5Ako_1830-1850 and half of the 3'-end of MpDWF5Ako_1830-1850/ MpDWF5Ako_1878-1897 were generated by PCR using pMD-gtRNA containing gRNA and tRNA scaffolds as a template and primer set containing restriction enzyme BsaI sites (MpDWF5Ako_1824-1843FW1 and MpDWF5Ako_1830-1850RV1, MpDWF5Ako_1830-1850FW2 and MpDWF5Ako_1878-1897RV2) (Supplementary Table S4). The units

containing two gRNAs–tRNAs were independently inserted into the BsaI site of the pMpGE_EnM01 vector using the Golden Gate Cloning method. pMpGE_EnM01 (Genbank accession number: LC716685) is the entry vector containing attL1, Mp*U6-1* promoter and tRNA fragments in front of the BsaI site, and gRNA and At*U6-26* 3' terminator and attL2 fragments after the BsaI site. To generate pMpGE_EnM01, the attL1-MpU6-1pro-tRNA-BsaI-BsaI-gRNA-AtU6-26ter-attL2 fragment was synthesized artificially and cloned into the pEX-K4J2 vector (Eurofins Genomics, Tokyo). The constructed units in pMpGE_EnM01 were introduced into the destination vector pMpGE010 (Sugano *et al.*, 2018) using LR clonaseII (Invitrogen). The vector control was constructed by introducing the pMpGE_EnM01 empty vector into pMpGE010 using the abovementioned method. The vectors were introduced into the regenerating thalli of Tak-1 via *A. tumefaciens* GV2260 and the transformants were selected with 10 mg/mL hygromycin B as previously described (Kubota *et al*., 2013). The genomic DNA was isolated from the transformants and amplified from the target region by PCR using MpDWF5A_ex3_genotypingFW2 and MpDWF5A_ex3_genotypingRV listed in Supplemental Table S4. The PCR product was used for sequencing the respective target sites with a Microchip Electrophoresis System for DNA/RNA Analysis MCE™-202 MultiNA (Shimadzu).

Complementation of Mpdwf5-ko by constitutive expression of MpDWF5A

The *MpDWF5A* ORF was amplified by PCR with PrimeSTAR MAX (Takara Bio Inc., Shiga, Japan) from synthesized *MpDWF5A* cDNA using primers listed in Supplementary Table S5. The amplified products were subcloned into pENTR/D-TOPO (Invitrogen) using In-fusion HD cloning kit (Takara Bio Inc., Shiga, Japan). The MpDWF5A ORF in pENTR/D-TOPO was introduced into the destination vector pMpGWB303 (Ishizaki *et al.*, 2015) using LR clonaseII (Invitrogen). The pMpGWB303-*MpDWF5A* vector in *A. tumefaciens* GV2260 was used for transformation of the *Mpdwaf5a-ko* line #47-2, and the transformants were selected with 0.5μM chlorsulfuron as previously described (Kubota *et al*., 2013). The genomic DNA was isolated from the transformants and amplified from the target region by PCR with KOD FX neo (TOYOBO) using MpDWF5Aox_gtpFW and MpDWF5Aox_gtpRV listed in Supplemental Table S5, confirming the introduction of the *MpDWF5A* expression cassette. The thalli area in *Mpdwf5a-ko*, the vector control, and *MpDWF5A-ox* lines at 28 days old of age was

calculated by analyzing the photo using the ImageJ software (National Institute of Health, https://imagej.nih.gov/ij/).

Morphological observation

The thalli area and weight were measured for 35 days to evaluate the growth rate of *Mpdwf5a-ko* and the vector control strains (Supplementary Figure S4). Each gemma of *Mpdwf5a-ko* and the vector control strains was placed on the dish (day 0), and the thalli were sampled each 7 days. They were placed on the square plastic petri dish (140 × 100 × 14.5 mm, Eiken Chemical Co., Ltd., Tokyo, Japan) lids so that the thalli do not overlap. The thalli were lightly pressed to the bottom of the petri dish, and a picture was taken. The thalli area was calculated by analyzing the photo using the ImageJ software (National Institute of Health, https://imagej.nih.gov/ij/). To characterize dwarfism observed in 28-day-old *Mpdwaf5a-ko* lines (#5-13, #32-5, and #47-2), their phenotypes (the thalli area, weight, and number of gemma cups) were compared to the vector control (Figures 5E, 5F, and 5G). For morphological observation of the thallus and cup of *Mpdwf5a-ko*, the thalli of 28-day-old *Mpdwf5a-ko* #47-2 and the control strain were used. The sections were made by hand slicing the thallus along the midrib.

Renaissance staining was performed as described (Furuya et al., 2022). The thalli were fixed in 3.7% formalin solution and were degassed by vacuum infiltration. For clearing and cell wall staining, samples were treated with the ClearSee solution [10% (w/v) xylitol, 15% (w/v) sodium deoxycholate, and 25% (w/v) urea] with 0.02% (v/v) SCRI Renaissance 2200 (Renaissance Chemicals, Selby, UK) (Kurihara *et al.* 2015). After replacing with the ClearSee solution, samples were kept for four additional days or more. For microscopic observations, samples were mounted on glass slides with the ClearSee solution; SCRI Renaissance 2200 fluorescence images were obtained using the confocal laser scanning microscope (Olympus FLUOVIEW FV1000, Tokyo, Japan) at excitation and detection wavelengths of 405 and 425–460 nm for SCRI Renaissance 2200 fluorescence, respectively. The thalli were sampled and soaked in 0.1 % 387 toluidine blue O for two minutes. The toluidine-blue-stained thalli were observed with an upright microscope after washed three times with sterilized water.

Feeding experiments with sterols and BRs

Fourteen-day-old *Mpdwf5a-ko* #47-2 and Tak-1 thalli were used for the castasterone feeding assay. Castasterone (1 mM) was dissolved in ethanol and diluted in two ways, 0.01 mM and 0.1 mM with ethanol. The 0, 0.01, 0.1, and 1 mM castasterone solutions were added to the half-strength Gamborg-B5 agar medium (diluted 1000-folds). The thalli were transferred onto the half-strength Gamborg-B5 agar medium, including castasterone at different concentrations (0, 0.01, 0.1, and 1 μM), incubated for 14 days, and the morphologies of thalli and cup were observed. The agar media including castasterone were changed every 4 days.

Feeding experiments with campesterol, stigmasterol, and 6-deoxocastasterone (1 μM each) dissolved in 0.09% (w/v) of 2-hydroxypropyl-β-cyclodextrin (FUJIFILM Wako Pure Chemical Co., Osaka, Japan) were performed using 10-day-old plants of *Mpdwf5a-ko* #47-2 and Tak-1. To prepare the feeding solution (1 μM each), campesterol, stigmasterol, and 6-deoxo-castasterone, 1 mM each, were dissolved in ethanol, 10 μL each were dried under nitrogen stream, and redissolved in 10 mL 0.09% (w/v) 2-hydroxypropyl-β-cyclodextrin. The 1 μM solutions and the mock solution (0.09% (w/v) 2-hydroxypropyl-β-cyclodextrin) were sterilized by filtration with Millex-GP (Merck Millipore Ltd., Cork Ireland). In the feeding experiments, the solution was layered over the entire thalli and removed after 5 min. This treatment was conducted every 4 days, and the phenotypes (thalli area, weight, and the number of cup) were observed after 18 days.

Data availability

The data underlying this article are available in the article and in its online supplementary material.

Funding

This research was supported in part by the grant “Program on Small Business Innovation Research” from the Project of the Bio-oriented Technology Research Advancement Institution (K.I. and M.M.).

Acknowledgments

We thank Brassino Co., Ltd. (Japan) for kindly providing castasterone.

Author contributions

M.H., and M.M. designed and planned the study. M.H., K.I., and M.M. performed the experiments and analyzed the data. R.A., and M.Y. helped in designing, executing, and interpreting the experiments and results. M.H., and M.M. wrote and edited the manuscript.

Disclosure

The authors declare no competing interests.

References

Bowman, J.L., Kohchi, T., Yamato, K.T., Jenkins, J., Shu, S., Ishizaki, K. *et al.* (2017) Insights into Land Plant Evolution Garnered from the Marchantia polymorpha Genome. *Cell* 171: 287-304.e15

Cannell, N., Emms, D.M., Hetherington, A.J., MacKay, J., Kelly, S., Dolan, L. *et al.* (2020) Multiple Metabolic Innovations and Losses Are Associated with Major Transitions in Land Plant Evolution. *Current Biology* 30: 1783-1800.e11

Carland, F., Fujioka, S. and Nelson, T. (2010) The Sterol Methyltransferases SMT1, SMT2, and SMT3 Influence *Arabidopsis* Development through Nonbrassinosteroid Products. *Plant Physiology* 153(2): 741–756

Choe, S., Tanaka, A., Noguchi, T., Fujioka, S., Takatsuto, S., Ross, A.S. *et al.* (2000) Lesions in the sterol Delta7 reductase gene of *Arabidopsis* cause dwarfism due to a block in brassinosteroid biosynthesis. *The Plant Journal* 21: 431–443

Choe, S., Noguchi, T., Fujioka, S., Takatsuto, S., Tissier, C.P., Gregory, B.D. *et al.* (1999a) The *Arabidopsis* dwf7 / ste1 Mutant Is Defective in the 7 Sterol C-5 Desaturation Step Leading to Brassinosteroid Biosynthesis. *The Plant Cell* 11: 207–221

Choe, S., Dilkes, B.P., Gregory, B.D., Ross, A.S., Yuan, H., Noguchi, T. *et al.* (1999b) The *Arabidopsis dwarf1* Mutant Is Defective in the Conversion of 24-Methylenecholesterol to Campesterol in Brassinosteroid Biosynthesis1. *Plant Physiology* 119: 897–908

Darnet, S., Blary, A., Chevalier, Q. and Schaller, H. (2021) Phytosterol Profiles, Genomes and Enzymes – An Overview. *Frontiers in Plant Science* 12: 665206

Dembitsky, V.M. (1993) Lipids of bryophytes. *Progress in Lipid Research 32*: 281–356

Demel, R.A. and de Kruyff, B. (1976) The function of sterols in membranes. *Biochimica et Biophysica Acta (BBA) - Reviews on Biomembranes* 457: 109–132

Diener, A.C., Li, H., Zhou, W., Whoriskey, W.J., Nes, W.D. and Fink, G.R. (2000) *STEROL METHYLTRANSFERASE 1* Controls the Level of Cholesterol in Plants. *The Plant Cell* 12: 853–870

Edgar, R.C. (2004) MUSCLE: a multiple sequence alignment method with reduced time and space complexity. *BMC Bioinformatics* 5: 113

Ferreira-Guerra, M., Marquès-Bueno, M., Mora-García, S., & Caño-Delgado, A. I. (2020). Delving into the evolutionary origin of steroid sensing in plants. *Current opinion in plant biology*, *57*: 87-95

Ferrer, A., Altabella, T., Arró, M. and Boronat, A. (2017) Emerging roles for conjugated sterols in plants. *Progress in Lipid Research* 67: 27–37

Furumizu, C. and Sawa, S. (2021) Insight into early diversification of leucine-rich repeat receptor-like kinases provided by the sequenced moss and hornwort genomes. *Plant Molecular Biology* 107: 337–353

Furuya, T., Nishihama, R., Ishizaki, K., Kohchi, T., Fukuda, H., & Kondo, Y. (2022). A glycogen synthase kinase 3-like kinase MpGSK regulates cell differentiation in *Marchantia polymorpha*. *Plant Biotechnology*, 39: 65-72.

Girard, J., Lanneau, G., Delage, L., Leroux, C., Belcour, A., Got, J. *et al.* (2021) Semi-Quantitative Targeted Gas Chromatography-Mass Spectrometry Profiling Supports a Late Side-Chain Reductase Cycloartenol-to-Cholesterol Biosynthesis Pathway in Brown Algae. *Frontiers in Plant Science* 12: 648426

Grandmougin-Ferjani, A., Schuler-Muller, I. and Hartmann, M.A. (1997) Sterol Modulation of the Plasma Membrane H+-ATPase Activity from Corn Roots Reconstituted into Soybean Lipids. *Plant Physiology* 113: 163–174

He, J. X., Gendron, J. M., Sun, Y., Gampala, S. S., Gendron, N., Sun, C. Q., Wang, Z. Y. (2005). BZR1 is a transcriptional repressor with dual roles in brassinosteroid homeostasis and growth responses. *Science*, *307*(5715), 1634-1638.

Ishizaki, K., Chiyoda, S., Yamato, K.T. and Kohchi, T. (2008) Agrobacterium-Mediated Transformation of the Haploid Liverwort Marchantia polymorpha L., an Emerging Model for Plant Biology. *Plant and Cell Physiology* 49: 1084–1091

Ishizaki, K., Nishihama, R., Ueda, M., Inoue, K., Ishida, S., Nishimura, Y. *et. al.* (2015) Development of Gateway Binary Vector Series with Four Different Selection Markers for the Liverwort *Marchantia polymorpha*. *PLOS ONE 10*(9), e0138876.

Jang, J.C., Fujioka, S., Tasaka, M., Seto, H., Takatsuto, S., Ishii, A. *et al.* (2000) A critical role of sterols in embryonic patterning and meristem programming revealed by the *fackel* mutants of *Arabidopsis thaliana*. *Genes & Development* 14: 1485–1497

Klahre, U., Noguchi, T., Fujioka, S., Takatsuto, S., Yokota, T., Nomura, T. *et al.* (1998) The *Arabidopsis DIMINUTO* / *DWARF1* Gene Encodes a Protein Involved in Steroid Synthesis. *The Plant Cell* 10: 1677–1690

Kodama K., Rich, K, M., Yoda, A., Shimazaki, S., Xie, X., Akiyama, K. *et al.* (2022) An Ancestral Function of Strigolactones as Symbiotic Rhizosphere Signals. *Nature Communications* 13: 3974

Kurihara, D., Mizuta, Y., Sato, Y. and Higashiyama, T. (2015) ClearSee: a Rapid Optical Slearing Reagent for Whole-plant Fluorescence Imaging. *Development* 142: 4168–4179.

Kubota, A., Ishizaki, K., Hosaka, M. and Kohchi, T. (2013) Efficient *Agrobacterium* -Mediated Transformation of the Liverwort *Marchantia polymorpha* Using Regenerating Thalli. *Bioscience, Biotechnology, and Biochemistry* 77: 167–172

Kumar, S., Stecher, G., Li, M., Knyaz, C. and Tamura, K. (2018) MEGA X: Molecular Evolutionary Genetics Analysis across Computing Platforms. *Molecular Biology and Evolution* 35: 1547–1549

Mecchia, M.A., García-Hourquet, M., Lozano-Elena, F., Planas-Riverola, A., Blasco-Escamez, D., Marquès-Bueno, M. *et al.* (2021) The BES1/BZR1-family transcription factor MpBES1 regulates cell division and differentiation in Marchantia polymorpha. *Current Biology* 31: 4860-4869.e8

Men, S., Boutté, Y., Ikeda, Y., Li, X., Palme, K., Stierhof, Y.D. *et al.* (2008) Sterol-dependent endocytosis mediates post-cytokinetic acquisition of PIN2 auxin efflux carrier polarity. *Nature Cell Biology* 10: 237–244

Nakajima, M., Miyazaki, S. and Kawaide, H. (2020) Hormonal Diterpenoids Distinct to Gibberellins Regulate Protonema Differentiation in the Moss *Physcomitrium patens*. *Plant and Cell Physiology* 61: 1861–1868

Ohnishi, T., Bancos, S., Watanabe, B., Fujita, S., Szatmari, M., Koncz, C., *et al.* (2006) C-23 Hydroxylation by Arabidopsis CYP90C1 and CYP90D1 reveals a new shortcut route in brassinosteroid biosynthesis. *Plant Cell* 18: 3275-3288.

585 Park, S.H., Han, K.S., Kim, T.W., Shim, J.K., Takatsuto, S., Yokota, T. *et al.* (1999) In vivo and in vitro conversion
586 of teasterone to typhasterol in cultured cells of marchantia polymorpha. *Plant and Cell Physiology* 40: 955–960
587
588 Roche, Y., Gerbeau‐Pissot, P., Buhot, B., Thomas, D., Bonneau, L., Gresti, J. *et al.* (2008) Depletion of
589 phytosterols from the plant plasma membrane provides evidence for disruption of lipid rafts. *The FASEB Journal*
590 22: 3980–3991
591
592 Schrick, K., Mayer, U., Horrichs, A., Kuhnt, C., Bellini, C., Dangl, J. *et al.* (2000) FACKEL is a sterol C-14
593 reductase required for organized cell division and expansion in *Arabidopsis* embryogenesis. *Genes & Development*
594 14: 1471–1484
595
596 Shimada, T.L., Shimada, T., Okazaki, Y., Higashi, Y., Saito, K., Kuwata, K. *et al.* (2019) HIGH STEROL ESTER
597 1 is a key factor in plant sterol homeostasis. *Nature Plants* 5: 1154–1166
598
599 Silvestro, D., Villette, C., Delecolle, J., Olse, C.E., Motawia, M.S., Geoffroy, P. *et al.* (2018) Vitamin D5 in
600 *Arabidopsis thaliana*. *Scientific Reports* 8: 16348
601
602 Sonawane, P. D., Pollier, J., Panda, S., Szymanski, J., Massalha, H., Yona, M., *et al*. (2016). Plant cholesterol
603 biosynthetic pathway overlaps with phytosterol metabolism. *Nature plants*, *3*(1), 1-13
604
605 Souter, M., Topping, J., Pullen, M., Friml, J., Palme, K., Hackett, R. *et al.* (2002) hydra Mutants of *Arabidopsis*
606 Are Defective in Sterol Profiles and Auxin and Ethylene Signaling. *The Plant Cell* 14: 1017–1031
607
608 Sugano, S.S., Nishihama, R., Shirakawa, M., Takagi, J., Matsuda, Y., Ishida, S. *et al.* (2018) Efficient
609 CRISPR/Cas9-based genome editing and its application to conditional genetic analysis in *Marchantia polymorpha*.
610 *PLoS ONE* 13: e0205117
611
612 Voshall, A., Christie, N.T.M., Rose, S.L., Khasin, M, van Etten, J.L., Markham, J.E. *et al.* (2021) Sterol
613 Biosynthesis in Four Green Algae: A Bioinformatic Analysis of the Ergosterol Versus Phytosterol Decision Point.
614 *Journal of Phycology* 57: 1199–1211
615
616 Wang, Z.Y., Nakano, T., Gendron, J., He J., Chen, M., Vafeados, D. *et al.* (2002) Nuclear-Localized BZR1 Mediates
617 Brassinosteroid-Induced Growth and Feedback Suppression of Brassinosteroid Biosynthesis. *Developmental Cell*
618 2: 505–513
619
620 Willemsen, V., Friml, J., Grebe, M., van den Toorn, A., Palme, K. and Scheres, B. (2003) Cell Polarity and PIN
621 Protein Positioning in *Arabidopsis* Require *STEROL METHYLTRANSFERASE1* Function. *The Plant Cell* 15: 612–
622 625
623

Xiao, A., Cheng, Z., Kong, L., Zhu, Z., Lin, S., Gao, G. *et al.* (2014) CasOT: a genome-wide Cas9/gRNA off-target searching tool. *Bioinformatics* 30: 1180–1182

Yin, Y., Wang, Z.Y., Mora-Garcia, S., Li, J., Yoshida, S., Asami, T. *et al*. (2002) BES1 Accumulates in the Nucleus in Response to Brassinosteroids to Regulate Gene Expression and Promote Stem Elongation. *Cell* 109: 181–191

Yokota, T., Ohnishi, T., Shibata, K., Asahina, M., Nomura, T., Fujita, T. *et al*. (2017) Occurrence of brassinosteroids in non-flowering land plants, liverwort, moss, lycophyte and fern. *Phytochemistry* 136: 46–55

Tables

Table 1. Sterol composition and contents in *M. polymorpha*.

Sterol composition and contents in 18-day-old thalli of *M. polymorpha* were analyzed. The values (μg/g FW) are presented as mean ± standard errors (SE) in triplicate.

μg/g FW	cholesterol	campesterol	stigmasterol	β-sitosterol
free	0.28 ± 0.02	28.1 ± 2.02	78.02 ± 4.13	4.08 ± 0.10
free + ester	0.29 ± 0.02	30.85 ± 0.88	81.90 ± 1.00	3.89 ± 0.30

Figure legends

Figure 1. The sterol biosynthetic pathways in *Saccharomyces cerevisiae* (yeast), *Arabidopsis thaliana*, and *Marchantia polymorpha*.

The black thick solid arrows indicate the Δ7-reduction steps catalyzed by Δ5, Δ7-sterol Δ7-reductase in plants. The black thin solid arrows indicate the single reaction steps catalyzed by the indicated enzymes (abbreviations for each enzyme in yeast and plants are summarized in Supplementary Table S1). The double-lined arrows indicate multiple reaction steps. In plants, 2,3-oxidosqualene is converted to cycloartenol, which is further converted to typical phytosterols, campesterol, sitosterol, and stigmasterol, and a bioactive brassinosteroid castasterone is biosynthesized from campesterol via 6-deoxocastasterone by CYP85A1. In yeast, 2,3-oxidosqualene is converted to lanosterol and further to ergosterol.

Figure 2. Sterol profile of *M. polymorpha*.

The extract from eighteen-day-old Tak-1 thalli was analyzed by the GC-MS method. GC-MS chromatograms were acquired from the MS scan mode monitored with *m/z* 50-700. STD represents the chromatogram of the authentic standards; 1: cholesterol, 2: campesterol, 3: stigmasterol, 4: β-sitosterol, and 5: 25-hydroxylcholesterol (internal standard).

Figure 3. Phylogenetic analysis of C7Rs by the neighbor-joining method.

The amino acid sequences of C7Rs were acquired from the Phytozome, NCBI, and Mapolbas database. The accession numbers of NCBI and the gene IDs acquired from the Phytozome and Mapolbase are shown in the parentheses after the species name. The numbers beside the nodes indicate the bootstrap values (in percentages of 1000 replicates). Alignment was done by MUSCLE.

Figure 4. GC-MS analysis of the sterol profile of *Mpdwf5a-ko.*

(A) The GC-MS chromatograms acquired from selected ion monitoring (SIM). Thirty-five-day-old *Mpdwf5a-ko* and vector control strains were extracted for the sterol analysis using GC-MS. The gray dot lines indicate the retention times of campesterol (1), stigmasterol (2), and sitosterol (3). The orange dot lines indicate the retention times of the Δ7-type sterols (4, 5, and 6) expected to be converted from the corresponding phytosterols in *M. polymorpha*. The arrows represent the expected conversion of the phytosterols to the corresponding Δ7-type sterols based on the retention time shift between 7-dehydrocholesterol and cholesterol. 25-hydroxy-cholesterol was added as the internal standard. 1: campesterol, 2: stigmasterol, 3: β-sitosterol, 4: Δ7-campesterol, 5: Δ7-stigmasterol, and 6: Δ7-β-sitosterol.

(B) The quantification of sterols of *Mpdwf5a-ko*. The sterol contents (μg/g FW) shown in Figure 6 were measured using the GC-MS chromatograms. The SIM chromatogram constructed calibration curve of 7-dehydrocholesterol with 25-hydroxycholesterol as the internal standard. The amount of each Δ7-type phytosterol was assigned as 7-dehydrocholesterol equivalent. The error bars represent the standard errors (SE). The mean and SE were calculated from three biological replicates.

Figure 5. The dwarf phenotype of *Mpdwf5a-ko*.

The phenotypes of the whole bodies were observed and photographed in in bright field using an optical microscope. A, the 28-day-old vector control; B, the 28-day-old *Mpdwf5a-ko* #47-2; C, the 56-day-old vector control; D the 72-day-old *Mpdwf5a-ko* #47-2. Comparison of the thalli area (E), weight (F), and number of cups (G) between the vector control and *Mpdwf5a-ko* was performed at twenty-eight days of age. The error bars represent standard errors (SE). The mean and SE were calculated for nine biological replicates. A *t*-test was performed, and data showing significant differences between the vector control and *Mpdwf5a-ko* are indicated by asterisks (*t*-test, ***. $p<0.001$). VC, vector control; #5, *Mpdwf5a-ko*#5-13; #32, *Mpdwf5a-ko*#32-5; #47, *Mpdwf5a-ko*#47-2

Figure 6. Microscopic observation of the morphological phenotypes of Mp*dwf5a-ko.*

The morphological phenotypes of the vector control (A, B, C) and *Mpdwf5a*-ko#47-2 (D, E, F) at 28 days of age were observed and photographed in bright field using an optical microscope. A and D, apical meristem in thallus; B and E, apical meristem section sliced along the midlib; C and F, gemma cup section. The blue triangles (B) indicate the ventral scales in the vector control. The red triangles (D and E) indicate the excessive formation of apical meristems in *Mpdwf5a*-ko#47-2. VC, the vector control; ko, *Mpdwf5a*-ko#47-2.

The thalli of the vector control (G) and *Mpdwf5a*-ko#47-2 (I) were stained with toluidine blue, and the schematic diagrams of G and I are H and J, respectively. The gray lines in H and J indicate rhizoids, and the red lines in H and J indicate anomalous tissues. Renaissance staining of the thallus of *Mpdwf5a*-ko#47-2 (K) was performed and observed using the confocal laser scanning microscope (K).

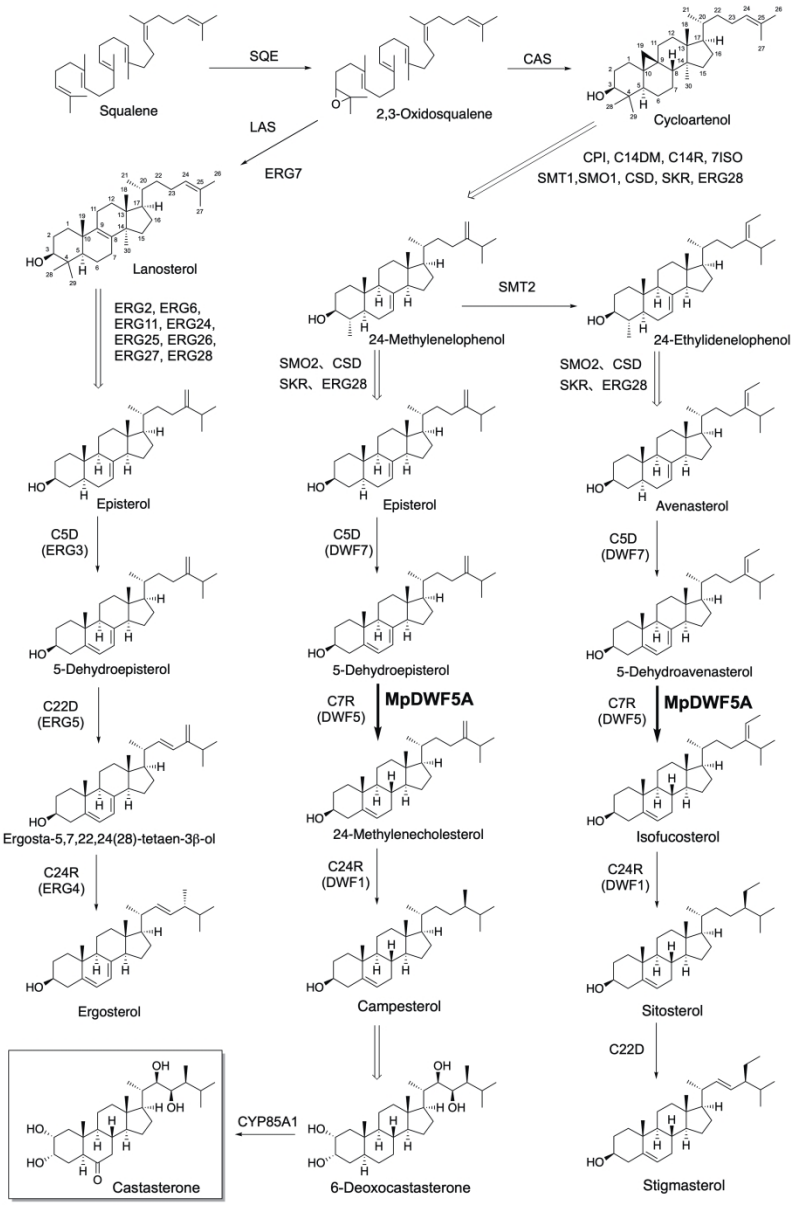

Figure 1. The sterol biosynthetic pathways in Saccharomyces cerevisiae (yeast), Arabidopsis thaliana, and Marchantia polymorpha.
The black thick solid arrows indicate the □7-reduction steps catalyzed by □5, □7-sterol □7-reductase in plants. The black thin solid arrows indicate the single reaction steps catalyzed by the indicated enzymes (abbreviations for each enzyme in yeast and plants are summarized in Supplementary Table S1). The double-lined arrows indicate multiple reaction steps. In plants, 2,3-oxidosqualene is converted to cycloartenol, which is further converted to typical phytosterols, campesterol, sitosterol, and stigmasterol, and a bioactive brassinosteroid castasterone is biosynthesized from campesterol via 6-deoxocastasterone by CYP85A1. In yeast, 2,3-oxidosqualene is converted to lanosterol and further to ergosterol.

282x428mm (300 x 300 DPI)

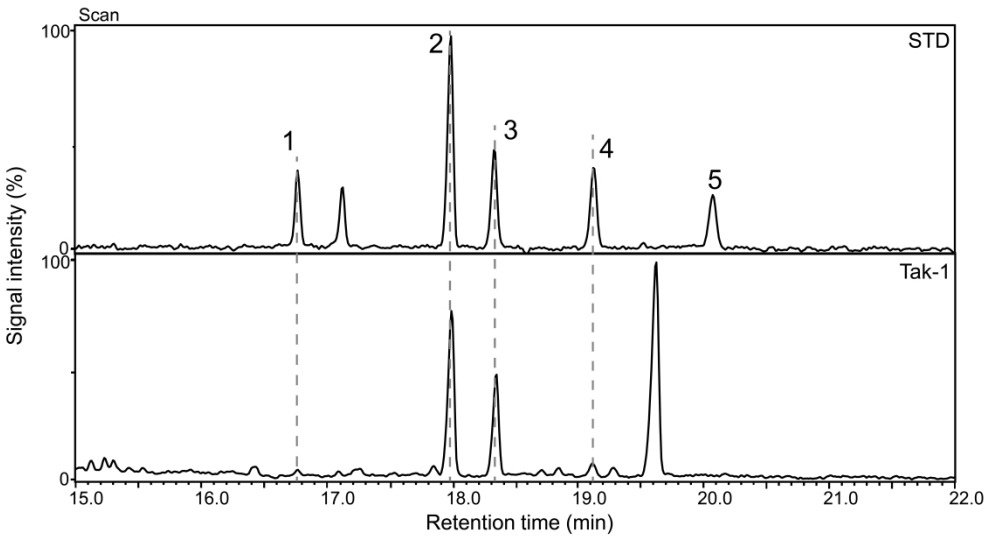

Figure 2. Sterol profile of M. polymorpha.
The extract from eighteen-day-old Tak-1 thalli was analyzed by the GC-MS method. GC-MS chromatograms were acquired from the MS scan mode monitored with m/z 50-700. STD represents the chromatogram of the authentic standards; 1: cholesterol, 2: campesterol, 3: stigmasterol, 4: β-sitosterol, and 5: 25-hydroxylcholesterol (internal standard).

178x97mm (1200 x 1200 DPI)

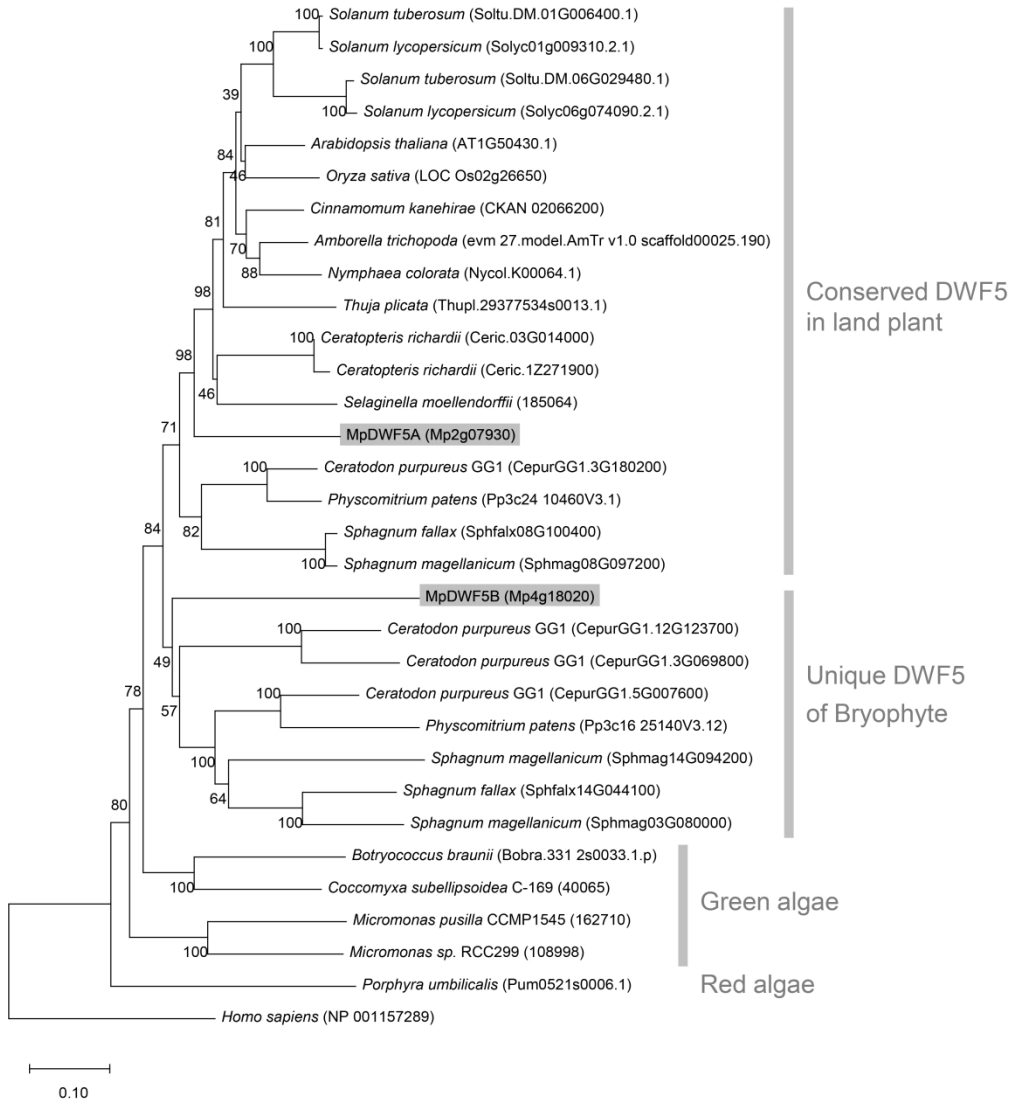

Figure 3. Phylogenetic analysis of C7Rs by the neighbor-joining method.
The amino acid sequences of C7Rs were acquired from the Phytozome, NCBI, and Mapolbas database. The accession numbers of NCBI and the gene IDs acquired from the Phytozome and Mapolbase are shown in the parentheses after the species name. The numbers beside the nodes indicate the bootstrap values (in percentages of 1000 replicates). Alignment was done by MUSCLE.

167x182mm (600 x 600 DPI)

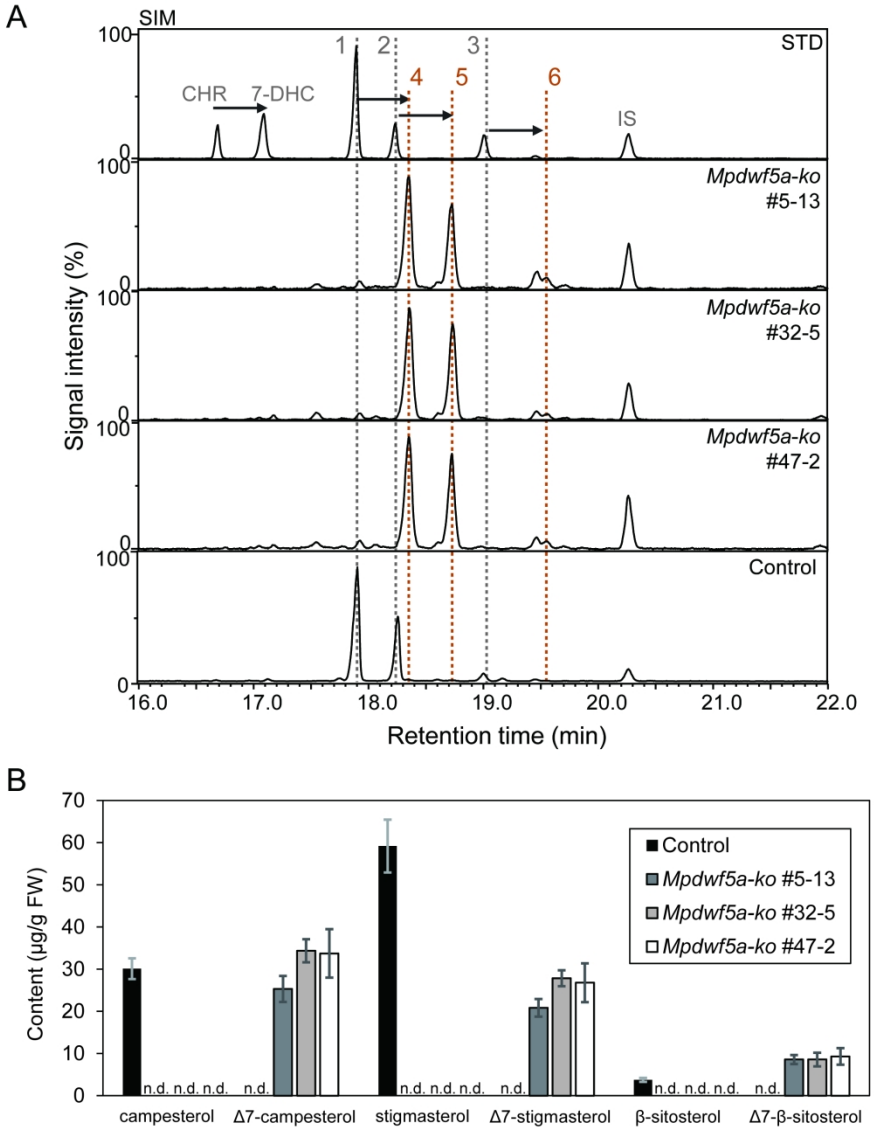

Figure 4. GC-MS analysis of the sterol profile of Mpdwf5a-ko.
(A) The GC-MS chromatograms acquired from selected ion monitoring (SIM). Thirty-five-day-old Mpdwf5a-ko and vector control strains were extracted for the sterol analysis using GC-MS. The gray dot lines indicate the retention times of campesterol (1), stigmasterol (2), and sitosterol (3). The orange dot lines indicate the retention times of the Δ7-type sterols (4, 5, and 6) expected to be converted from the corresponding phytosterols in M. polymorpha. The arrows represent the expected conversion of the phytosterols to the corresponding Δ7-type sterols based on the retention time shift between 7-dehydrocholesterol and cholesterol. 25-hydroxy-cholesterol was added as the internal standard. 1: campesterol, 2: stigmasterol, 3: β-sitosterol, 4: Δ7-campesterol, 5: Δ7-stigmasterol, and 6: Δ7-β-sitosterol.
(B) The quantification of sterols of Mpdwf5a-ko. The sterol contents (□g/g FW) shown in Figure 6 were measured using the GC-MS chromatograms. The SIM chromatogram constructed calibration curve of 7-dehydrocholesterol with 25-hydroxycholesterol as the internal standard. The amount of each Δ7-type phytosterol was assigned as 7-dehydrocholesterol equivalent. The error bars represent the standard errors (SE). The mean and SE were calculated from three biological replicates.

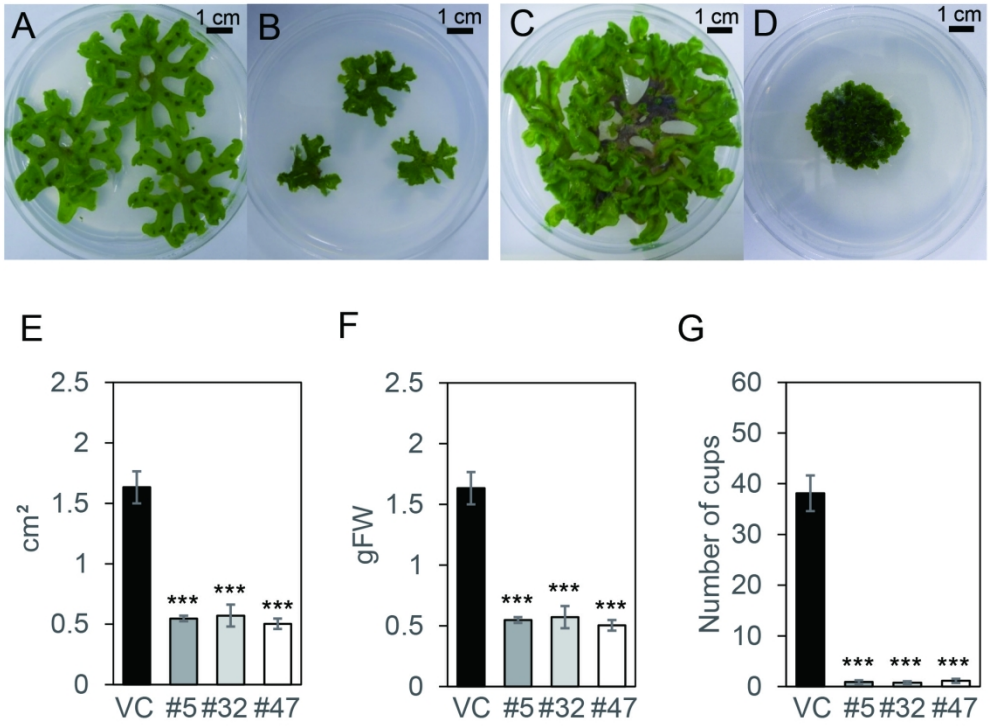

Figure 5. The dwarf phenotype of Mpdwf5a-ko.
The phenotypes of the whole bodies were observed and photographed in in bright field using an optical microscope. A, the 28-day-old vector control; B, the 28-day-old Mpdwf5a-ko #47-2; C, the 56-day-old vector control; D the 72-day-old Mpdwf5a-ko #47-2. Comparison of the thalli area (E), weight (F), and number of cups (G) between the vector control and Mpdwf5a-ko was performed at twenty-eight days of age. The error bars represent standard errors (SE). The mean and SE were calculated for nine biological replicates. A t-test was performed, and data showing significant differences between the vector control and Mpdwf5a-ko are indicated by asterisks (t-test, ***. $p<0.001$). VC, vector control; #5, Mpdwf5a-ko#5-13; #32, Mpdwf5a-ko#32-5; #47, Mpdwf5a-ko#47-2

175x131mm (300 x 300 DPI)

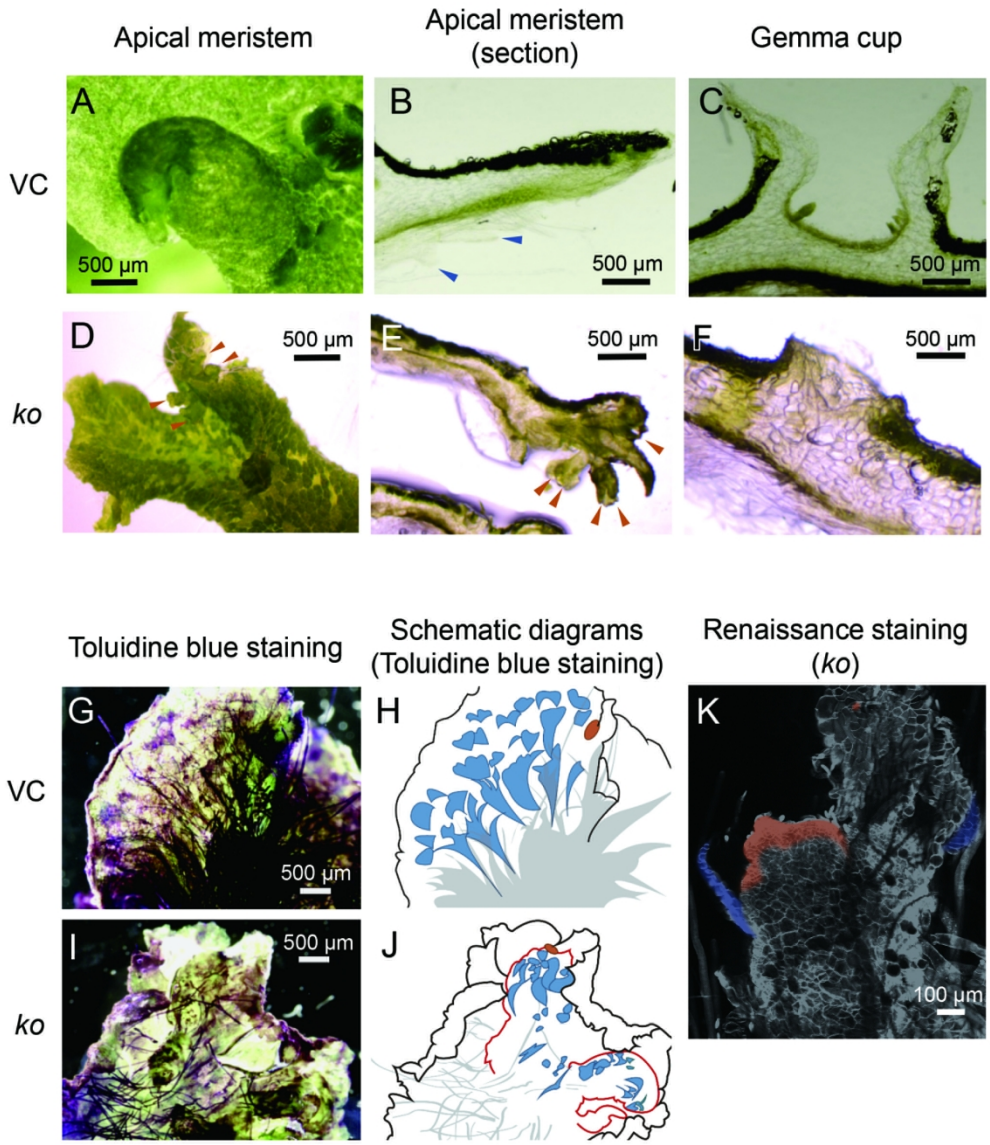

Figure 6. Microscopic observation of the morphological phenotypes of Mpdwf5a-ko.
The morphological phenotypes of the vector control (A, B, C) and Mpdwf5a-ko#47-2 (D, E, F) at 28 days of age were observed and photographed in bright field using an optical microscope. A and D, apical meristem in thallus; B and E, apical meristem section sliced along the midlib; C and F, gemma cup section. The blue triangles (B) indicate the ventral scales in the vector control. The red triangles (D and E) indicate the excessive formation of apical meristems in Mpdwf5a-ko#47-2. VC, the vector control; ko, Mpdwf5a-ko#47-2.
The thalli of the vector control (G) and Mpdwf5a-ko#47-2 (I) were stained with toluidine blue, and the schematic diagrams of G and I are H and J, respectively. The gray lines in H and J indicate rhizoids, and the red lines in H and J indicate anomalous tissues. Renaissance staining of the thallus of Mpdwf5a-ko#47-2 (K) was performed and observed using the confocal laser scanning microscope (K).

175x205mm (300 x 300 DPI)

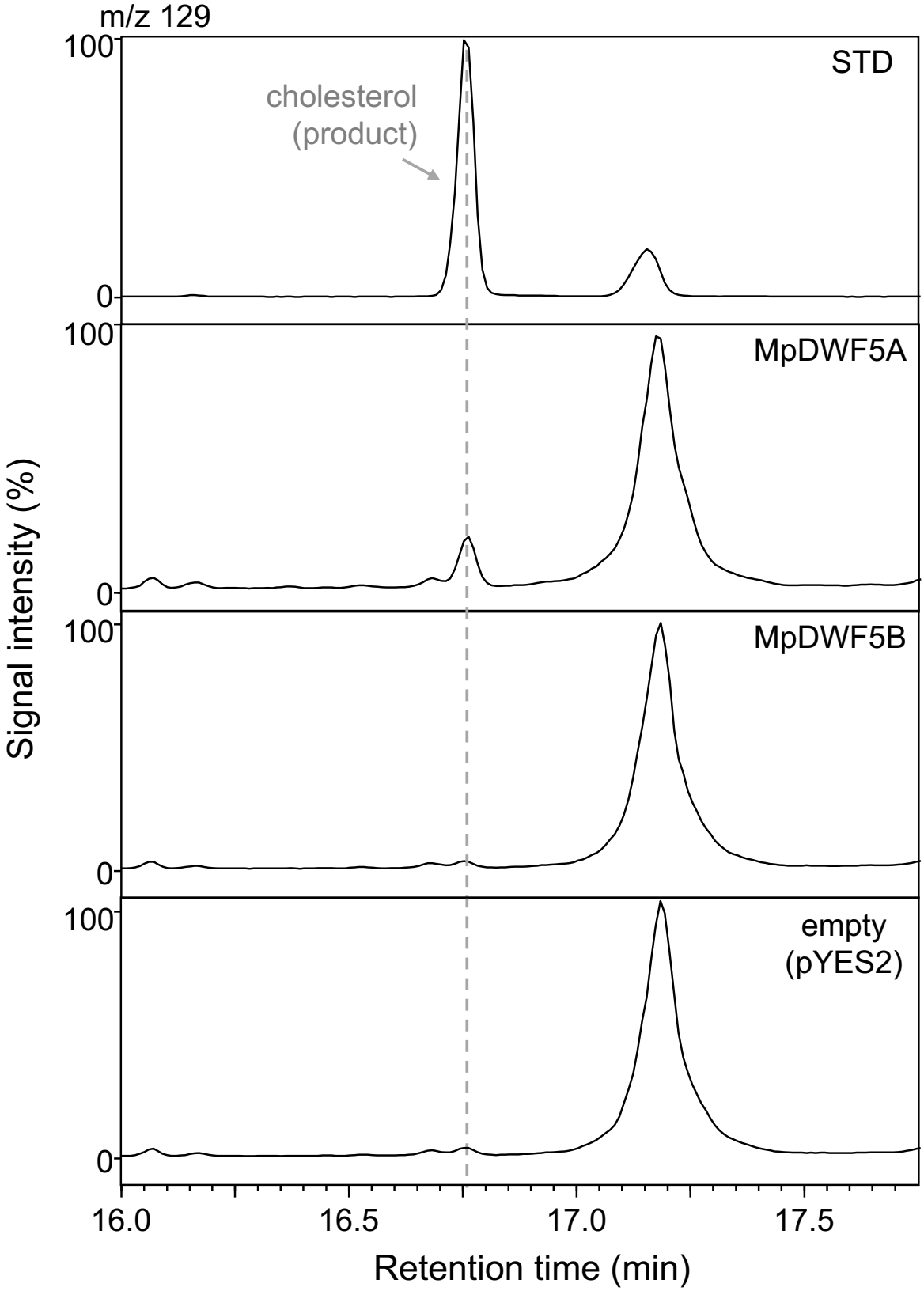

Supplementary Figure S1. *In vitro* assay of C7R activity in yeast.
The *in vitro* assay of the recombinant MpDWF5A and MpDWF5B expressed in yeast cells was performed with 7-dehydrocholesterol as a substrate, and GC-MS was used to analyze the reaction mixtures. The traces were extracted from the ion chromatograms at *m/z* 129. The dot line indicates the retention time of the reaction product, cholesterol.

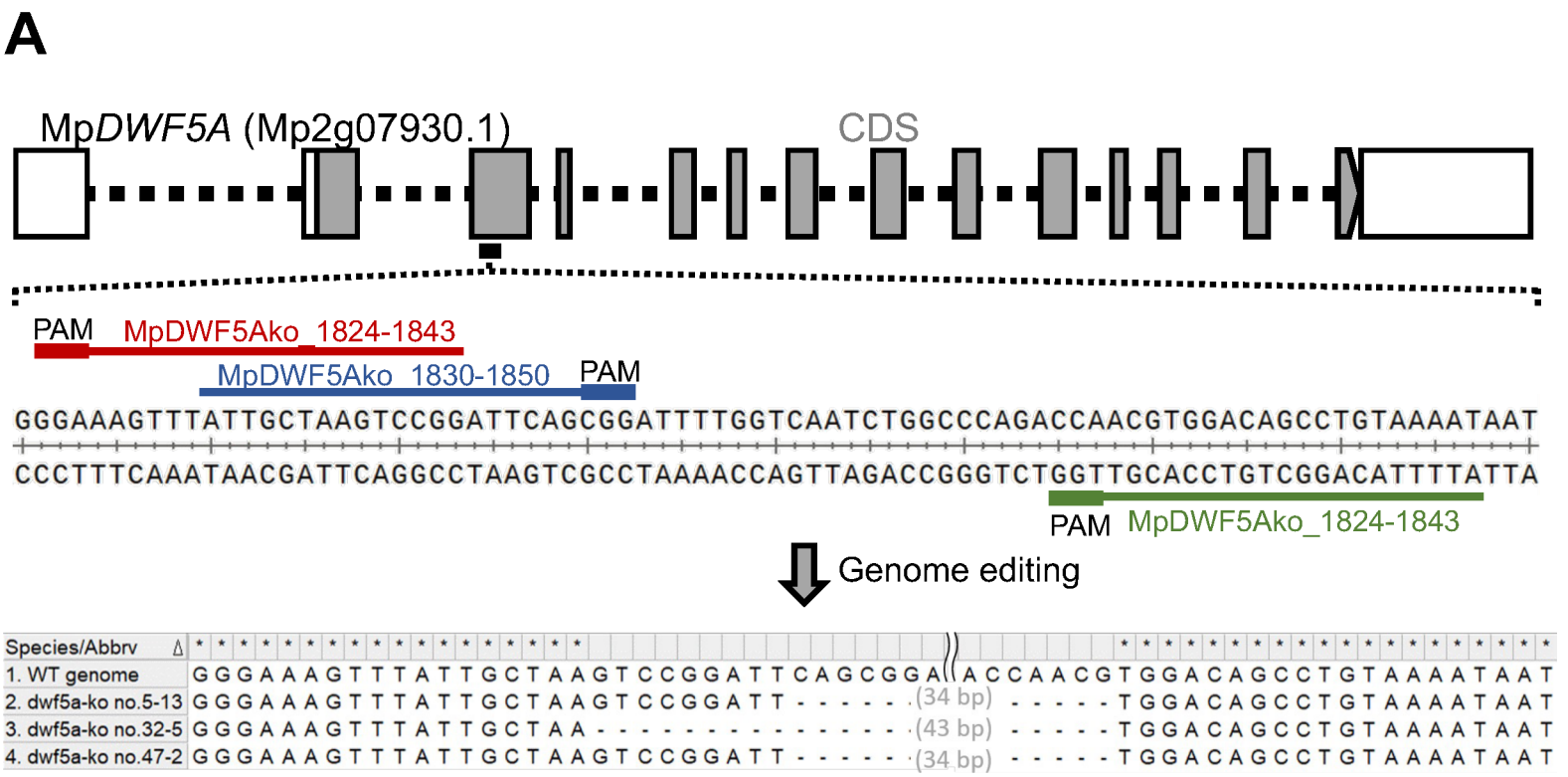

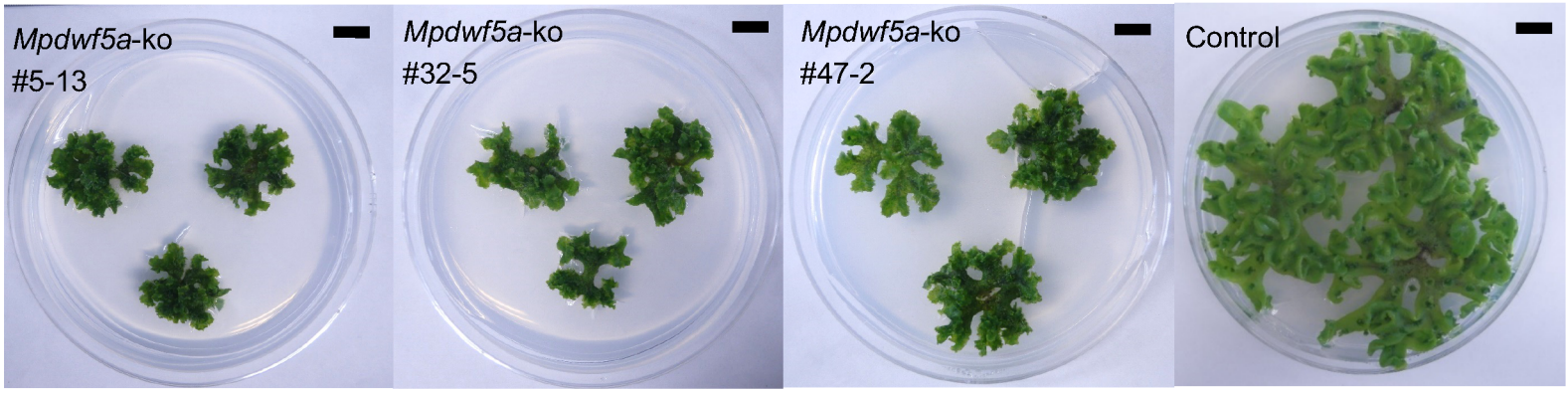

Supplementary Figure S2. Genome editing of *MpDWF5A*

(A) The target sites for *MpDWF5A*. The color-coded lines indicate the gRNA target sites and PAM sequences, respectively. The gRNA target sites were MpDWF5Ako_1824-1843 (red line), MpDWF5Ako_1830-1850 (blue line), and MpDWF5Ako_1878-1897 (green line), respectively. The gray boxes and white boxes indicate the CDS and untranslated regions. The dot black line indicates introns. The deletion of nucleotides is indicated as the dash, and the numbers of the deleted sequences are shown in the parentheses. The sequences of WT and edited *Mpdwf5a-ko* are shown at the bottom.

(B) The morphological phenotypes were observed in the *Mpdwf5a*-ko lines (28-day-old): #5-13, #32-15, and #47-2 generated by genome editing. Scale bars represent 1 cm.

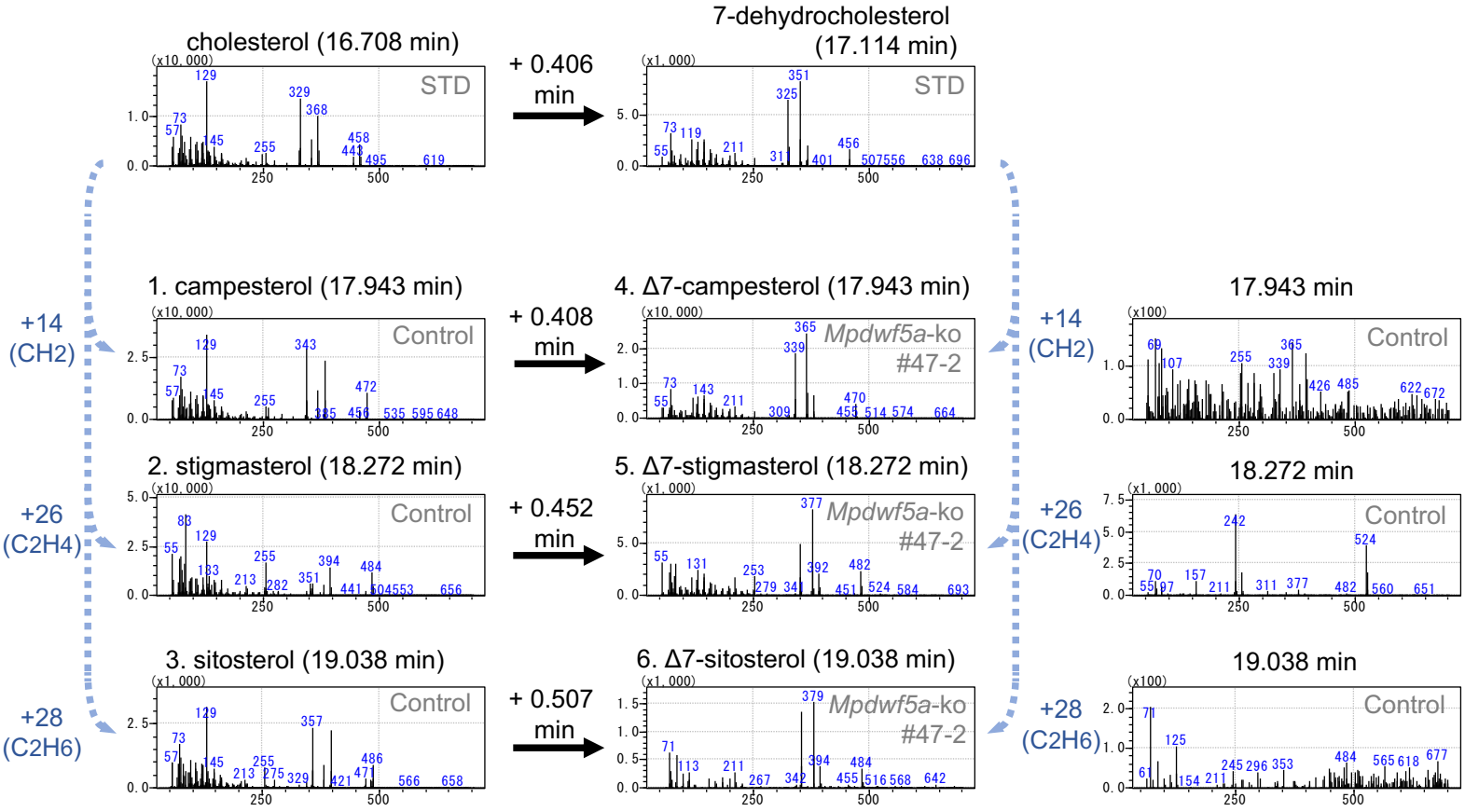

Supplementary Figure S3. MS spectra of the sterols in *Mpdwf5a-ko*.
The MS spectra of the authentic trimethylsilylated standards (cholesterol, campesterol, sitosterol, and stigmasterol) and the sterols accumulated in the *Mpdwf5a-ko* #47-2 line (35-day-old) were obtained by GC-MS. The retention time of each compound is shown at the top of the MS spectrum. The light blue dot arrows indicate the shifting of the m/z values of molecular and qualifier ions. The black arrows indicate the retention time-shifting.

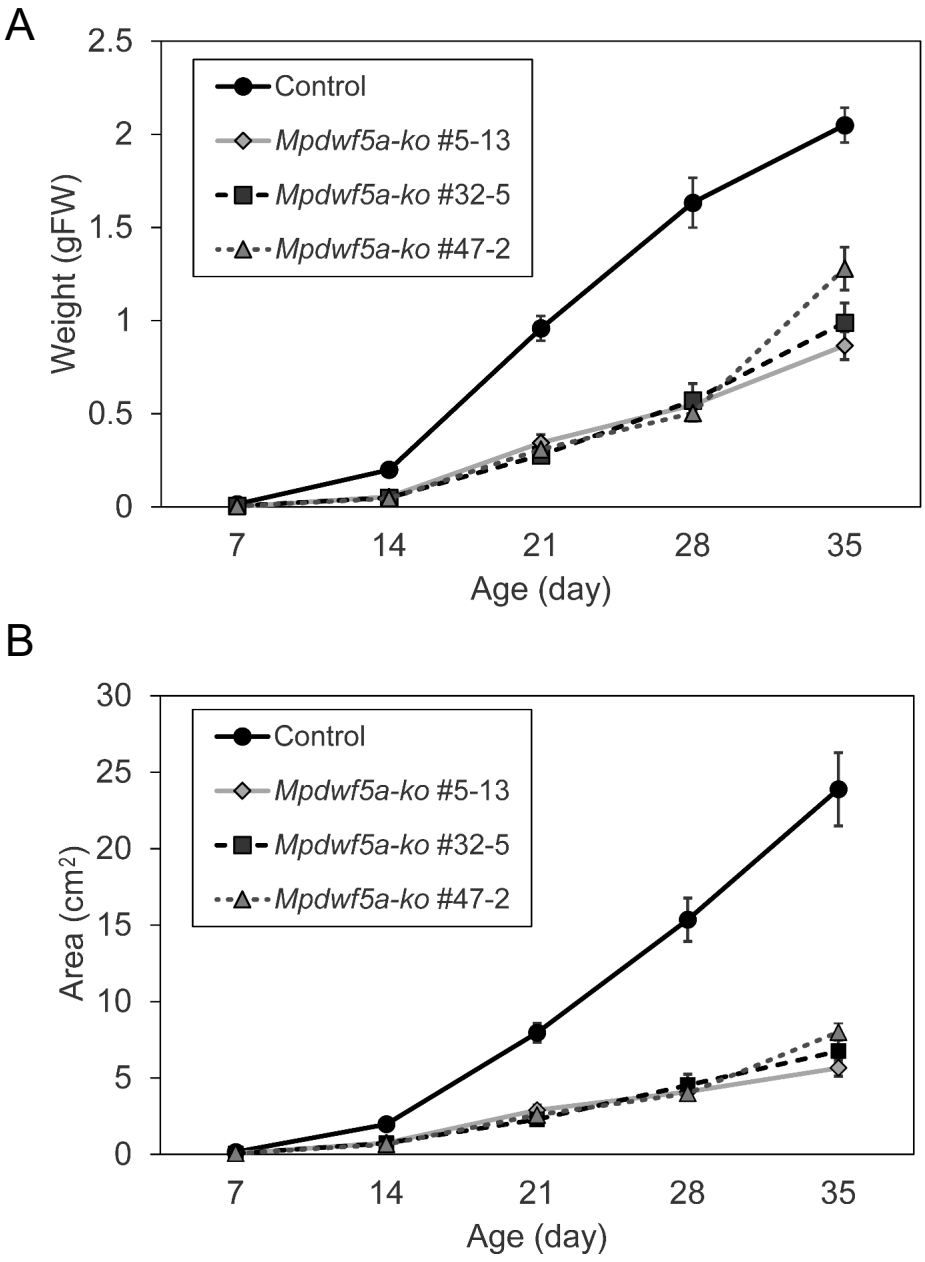

Supplementary Figure S4. Comparison of the growth rate between *Mpdwf5a-ko* and the vector control. The growth rates of *Mpdwf5a-ko* lines (#5-13, #32-5 and #47-2) and the vector control were assessed over a five-week period by analyzing the weight (A) and the area (B) of the thalli on a weekly basis. The error bars represent standard errors (SE). The mean and SE were calculated for nine biological replicates.

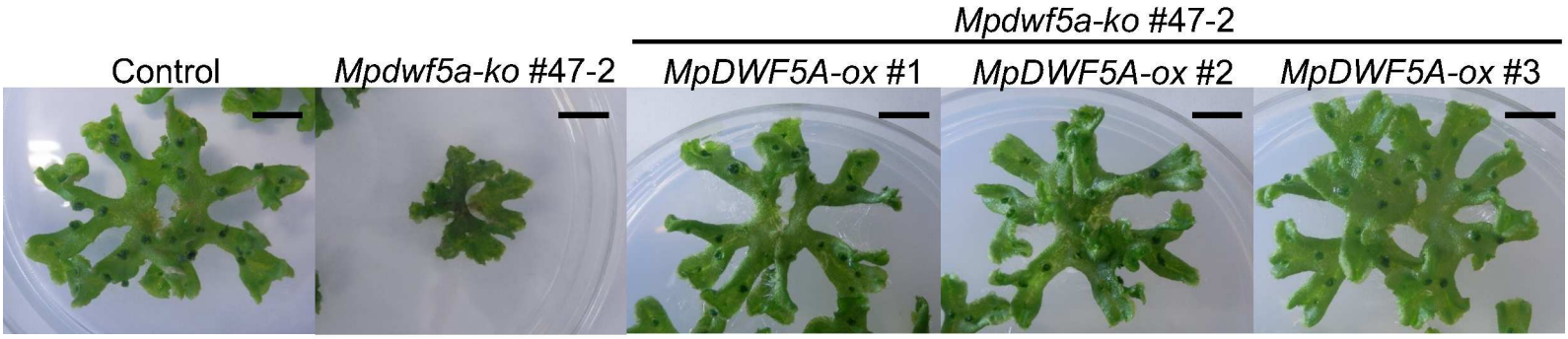

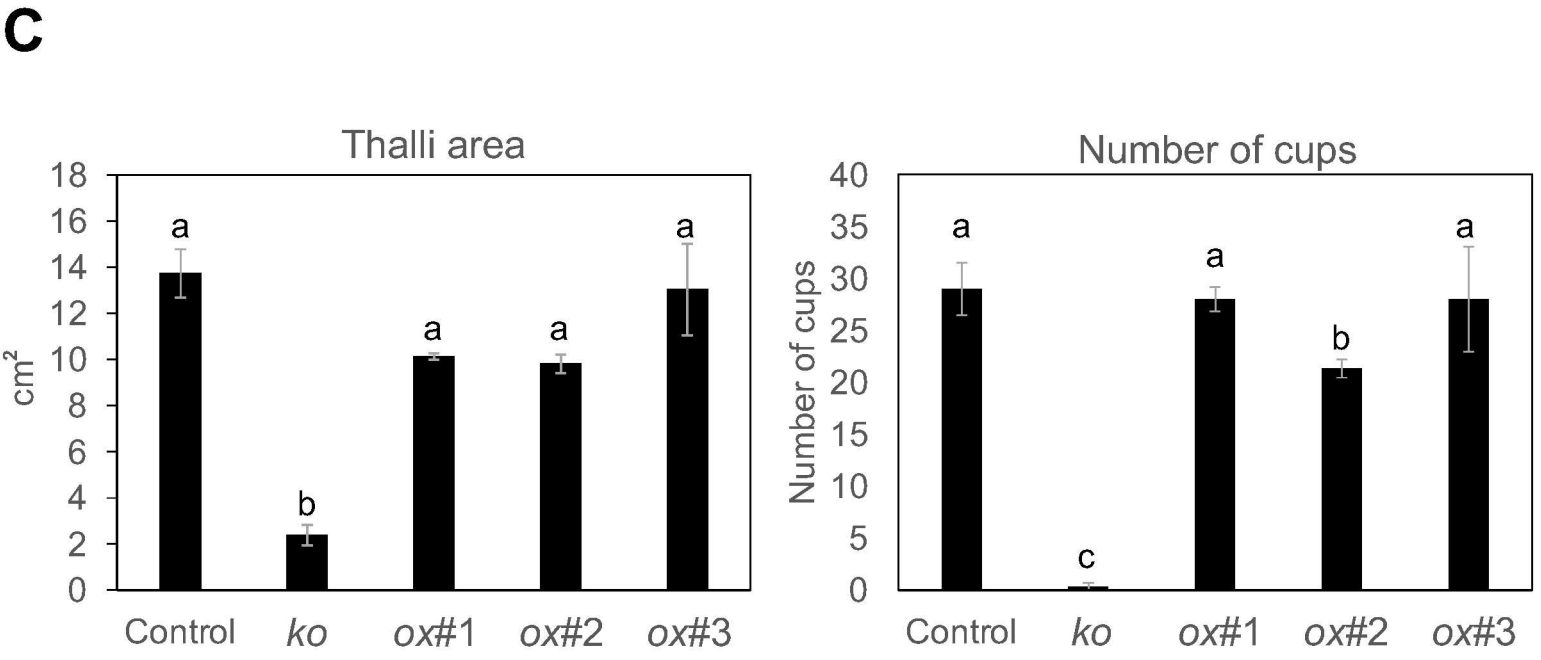

Supplementary Figure S5. Complementation of *Mpdwf5a-ko* by constitutive expression of *MpDWF5A*.
(A) The morphological phenotypes of the *MpDWF5A-ox* lines (28-day-old): #1, #2, and #3 were compared with the vector control (Control) and *Mpdwf5a-ko* #47-2. Scale bars represent 1 cm.
(B) The genotyping of *MpDWF5A-ox* lines by agarose gel electrophoresis. Lane1: *Mpdwf5a-ko* #47-2/*MpDWF5A*-ox #1, Lane2: *Mpdwf5a-ko* #47-2/*MpDWF5A*-ox #2, Lane3: *Mpdwf5a-ko* #47-2/*MpDWF5A*-ox #3, Lane4: positive control, the MpDWF5A/pMpGWB303 vector, Lane5: *Mpdwf5a*-ko #47-2
(C) Effects of constitutive expression of *MpDWF5A* on the thalli area and number of cups. The thalli area and number of cups of *Mpdwf5a-ko*, vector control, and *MpDWF5A-ox* lines (28-day-old) are shown as means ± standard error of three replicates. Significant differences were identified using a one-way analysis of variance (ANOVA) ($P < 0.05$, Tukey' tests). Different lowercase letters indicate significant differences between transgenic lines and control lines. Control: vector control, *ko*: *Mpdwf5a-ko* #47-2, *ox*#1: *Mpdwf5a-ko* #47-2/*MpDWF5A-ox* #1, *ox*#2: *Mpdwf5a-ko* #47-2/*MpDWF5A-ox* #2, *ox*#3: *Mpdwf5a-ko* #47-2/*MpDWF5A-ox* #3.

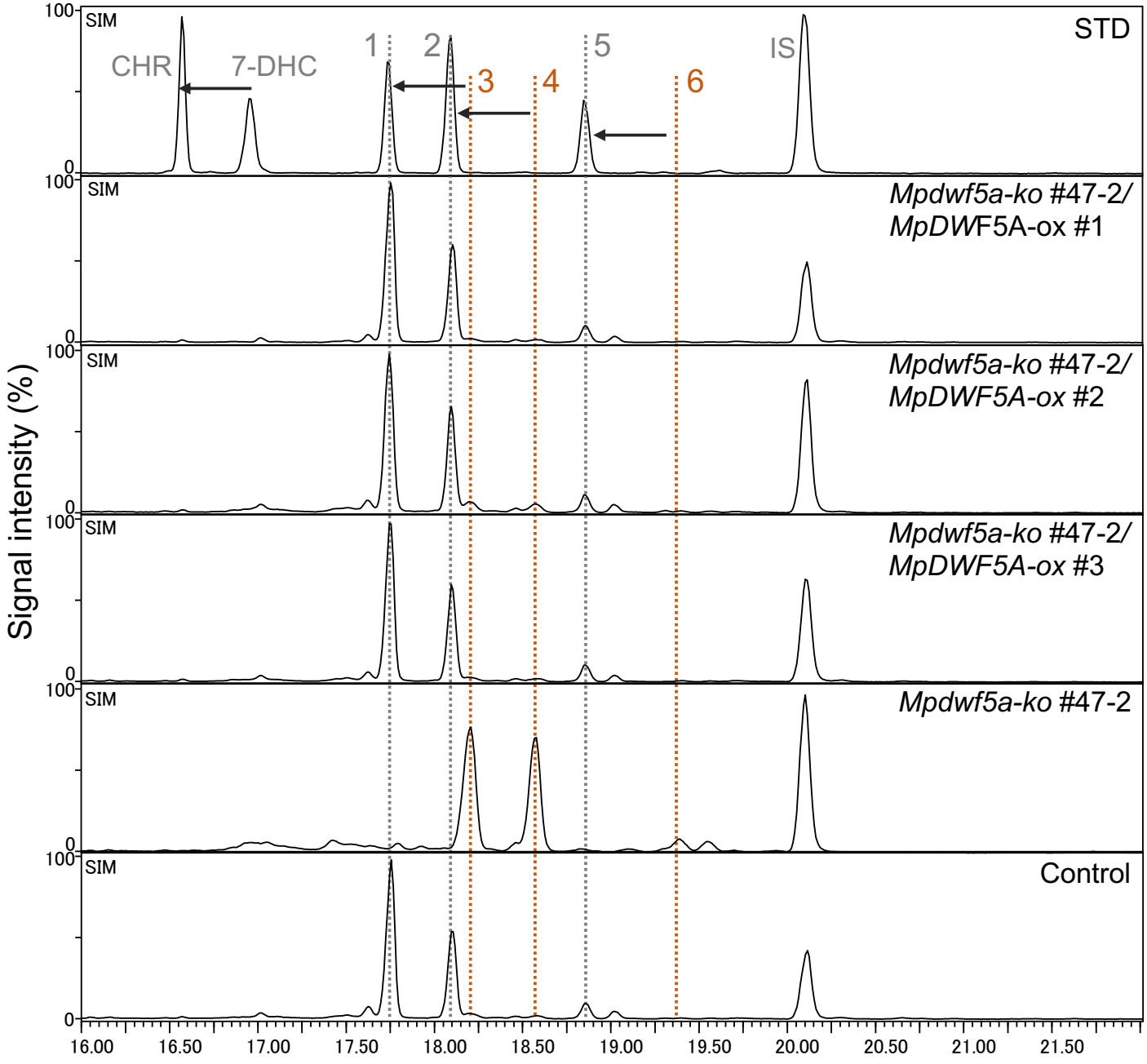

Supplementary Figure S6. Sterol profiles of *MpDWF5A-ox* lines.
GC-MS chromatograms acquired from selected ion monitoring (SIM). Twenty-eight-day-old the *MpDWF5A-ox* lines were used for the sterol analysis using GC-MS. The gray dot lines indicate the retention times of campesterol (1), stigmasterol (2), and sitosterol (3). The orange dot lines indicate the retention times of the Δ7-type sterols (4, 5, and 6) accumulated in *Mpdwf5a*-ko. The arrows represent the expected conversion of the phytosterols from the corresponding Δ7-type sterols based on the retention time shift between 7-dehydrocholesterol and cholesterol. 25-hydroxy-cholesterol was added as the internal standard. 1: campesterol, 2: stigmasterol, 3: β-sitosterol, 4: Δ7-campesterol, 5: Δ7-stigmasterol, and 6: Δ7-β-sitosterol.

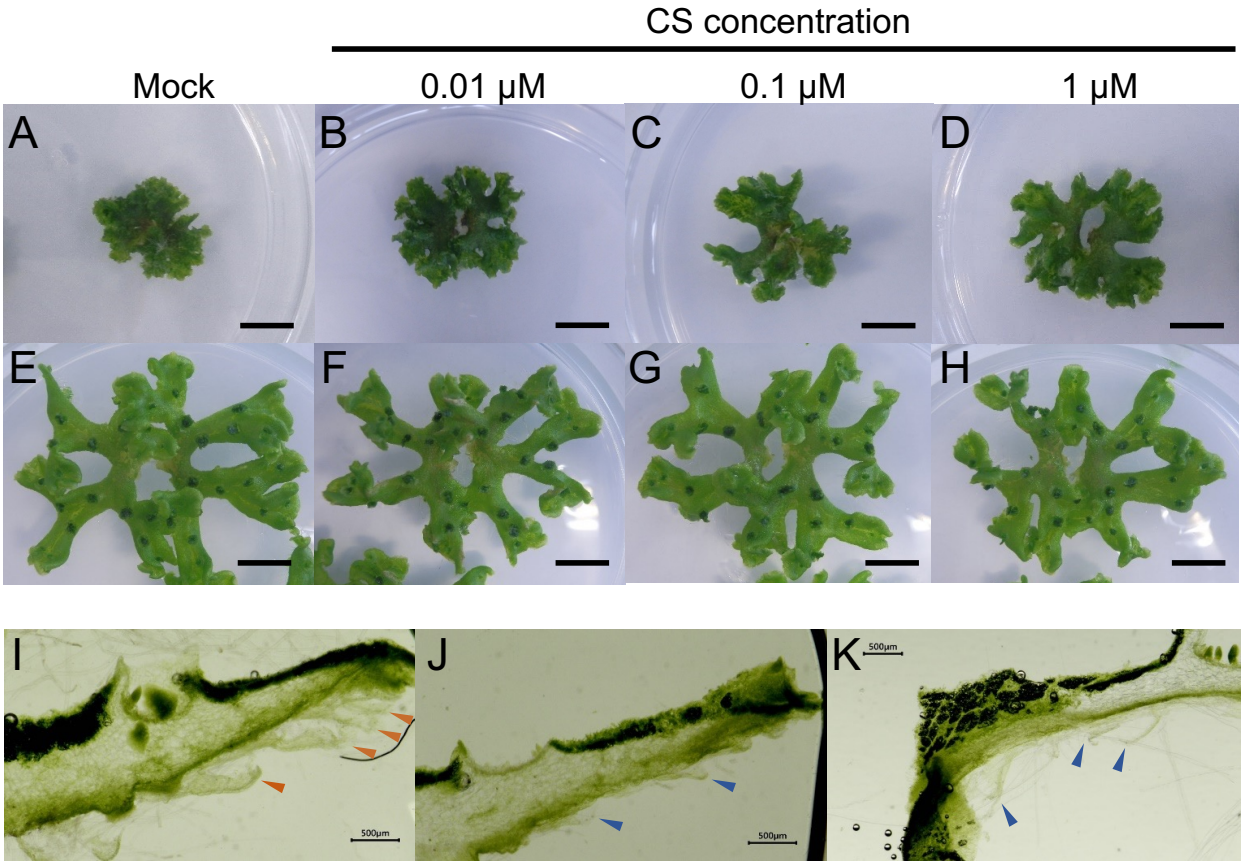

Supplementary Figure S7. Examination of the feeding rescue of *Mpdwf5a-ko* by castasterone.
Fourteen-day-old *Mpdwf5a-ko* #47-2 and Tak-1 thalli were grown in the half-strength Gamborg-B5 agar medium, including castasterone (CS) for 14 days. The CS concentration in the medium was adjusted to 0, 0.01, 0.1, and 1 µM. A–D, *Mpdwf5a-ko* #47-2; E–H, Tak-1 as the control. I, *Mpdwf5a-ko* #47-2 apical section of CS (0 µM) feeding. J, *Mpdwf5a-ko* #47-2 thallus apical section of 1 µM CS feeding. K, control thallus apical section of CS (0 µM) feeding. The red triangles (I) indicate the formation of abnormal meristem instead of the ventral scale in *Mpdwf5a-ko* #47-2. The blue triangles (J and K) indicate the formation of the ventral scale. A–H: scale bar = 1cm.

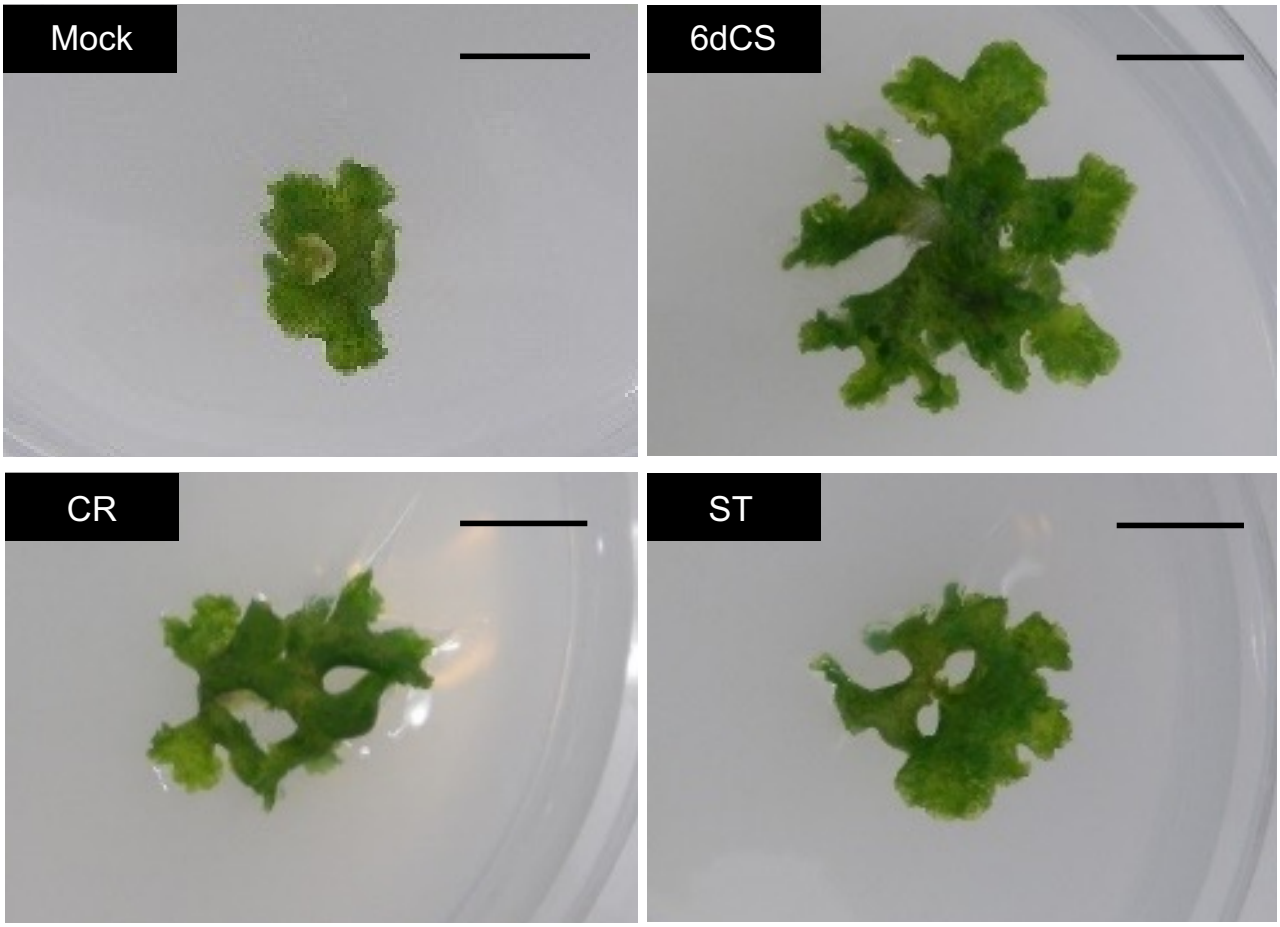

Supplementary Figure S8. Effects of feeding rescue by campesterol, stigmasterol, and 6-deoxocastasterone on the *Mpdwf5a-ko* mutant.

The phenotypes of 28-day-old *Mpdwf5a-ko* #47-2 fed with campesterol (CR), stigmasterol, (ST), and 6-deoxocastasterone (6dCS) are shown. In the feeding experiments, the solution (1 μM each in 0.09% 2-hydroxypropyl-β-cyclodextrin) was layered over the entire thalli (ten-day-old) and removed after 5 min. This treatment was conducted every 4 days, and the phenotypes were observed after 18 days. Mock indicates the treatment with 0.09% 2-hydroxypropyl-β-cyclodextrin alone. Scale bars indicate 1 cm.

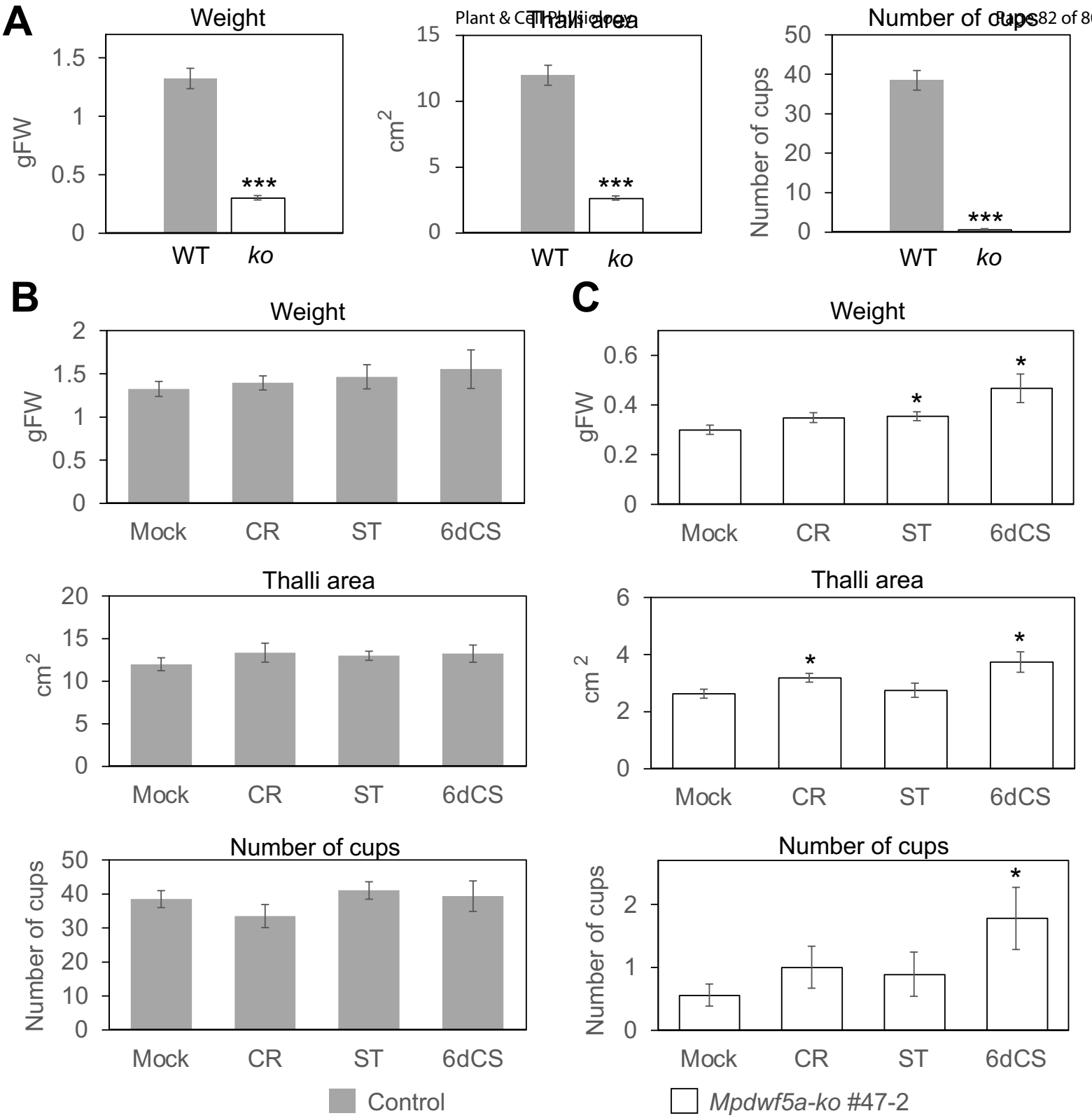

Supplementary Figure S9. Quantitative analysis of the effects of feeding rescue by campesterol, stigmasterol, and 6-deoxocastasterone on the phenotypes (thalli area, weight, and the number of cup) of *Mpdwf5a-ko*.

The phenotypes of 28-day-old *Mpdwf5a-ko* #47-2 fed with campesterol (CR), stigmasterol, (ST), and 6-deoxocastasterone (6dCS) are shown. In the feeding experiments, the solution (1 μM each in 0.09% 2-hydroxypropyl-β-cyclodextrin) was layered over the entire thalli (10-day-old) and removed after 5 min. This treatment was conducted every 4 days, and the phenotypes (thalli area, weight, and the number of cup) were observed after 18 days. Mock indicates the treatment with 0.09% 2-hydroxypropyl-β-cyclodextrin alone. The mean and SE were calculated for nine biological replicates.

(A) Comparison of the thalli area, weight, and number of cups between WT (Tak-1) and *ko* (*Mpdwf5a-ko* #47-2) thalli. The error bars represent standard errors (SE). The mean and SE were calculated for nine biological replicates.

A *t*-test was performed, and a line was drawn between the data that showed a significant difference (*t*-test, $p<0.001$). (B) Effects of feeding rescue with the compounds on the phenotypes (the thalli area, weight, and number of cups) of WT (Tak-1). (C) Effects of feeding rescue with the compounds on the phenotypes (the thalli area, weight, and number of cups) of *Mpdwf5a-ko* #47-2. A *t*-test was performed, and a line was drawn between the data that showed a significant difference (*t*-test, $p<0.05$).